Open Biomedical Network Benchmark

A Python Toolkit for Benchmarking Datasets with Biomedical Networks

Renming Liu
Michigan State University
liurenmi@msu.edu

Arjun Krishnan*
University of Colorado Anschutz Medical Campus
arjun.krishnan@cuanschutz.edu

Abstract

Over the past decades, network biology has been a major driver of computational methods developed to better understand the functional roles of each gene in the human genome in their cellular context. Following the application of traditional semi-supervised and supervised machine learning (ML) techniques, the next wave of advances in network biology will come from leveraging graph neural networks (GNN). However, to test new GNN-based approaches, a systematic and comprehensive benchmarking resource that spans a diverse selection of biomedical networks and gene classification tasks is lacking. Here, we present the Open Biomedical Network Benchmark (OBNB), a collection of node-classification benchmarking datasets derived using networks from 15 sources and tasks that include predicting genes associated with a wide range of functions, traits, and diseases. The accompanying Python package, `obnb`, contains reusable modules that enable researchers to download source data from public databases or archived versions and set up ML-ready datasets that are compatible with popular GNN frameworks such as PyG and DGL. Our work lays the foundation for novel GNN applications in network biology. `obob` will also help network biologists easily set-up custom benchmarking datasets for answering new questions of interest and collaboratively engage with graph ML practitioners to enhance our understanding of the human genome. OBNB is released under the MIT license and is freely available on GitHub: https://github.com/krishnanlab/obnb

1 Introduction

Life is orchestrated by remarkably complex interactions between biomolecules, such as genes and their products. Network biology [6, 7, 43, 93] has demonstrated remarkable success over the past two decades in systematically uncovering genes' functions and their relations to human traits and diseases. Accurately identifying genes associated with a particular disease, for example, is a vital step towards understanding the biological mechanisms underlying the condition, which in turn could lead to novel and effective diagnostic and treatment strategies [96, 51]. Early work in network biology focused on network diffusion-type methods based on the *guilt-by-association* principle [69], which states that genes interacting with each other likely participate in the same biological functions or pathways. The performance of these methods has subsequently been improved by the application of supervised learning [67]. In this trajectory, the next wave of improvements in network biology is likely to emanate from the surge of powerful graph machine learning (ML) techniques such as graph embeddings [27, 14] and graph neural networks [100, 106]. These methods have shown promising results in many graph-structured tasks, such as social networks [34], and have started to attract researchers to apply them to biological tasks [5, 104, 68]. To this end, accelerating the development and application of graph ML methods in network biology is of great importance.

However, there is a critical need for standardized benchmarks that allow reliable and reproducible assessment of the novel graph ML methods [81, 34]. Recent efforts such as MoleculeNet [99] and

Preprint. Under review.

Therapeutics Data Commons [37] for molecular and therapeutics property predictions, and Benchmarking GNN [23] and Open Graph Benchmark [34, 35] for more general graph benchmarks, have proven valuable in advancing the field of graph ML by providing carefully-constructed benchmarking datasets for applying specialized methods. Meanwhile, such comprehensive benchmarking datasets and systems are currently lacking for network biology. Furthermore, setting up ML-ready datasets for network biology is incredibly tedious. Some necessary steps include converting gene identifiers (IDs), setting up labeled data from annotated biomedical ontologies, filtering labeled data based on network gene coverage, and constructing realistic data splits mimicking real-world biologically meaningful scenarios. As a result, despite the remarkable amount of publicly available data for biomedical networks [36, 44] and annotations [82], the only widely available ML-ready datasets for network biology are `PPI` dataset from OhmNet [108] and `PPA` from the Open Graph Benchmark [34].

Contributions In this work, we address this critical need. Our main contributions are as follows:

1. We present a Python package `obnb` that provides reusable modules for data downloading, processing, and split generation to set up node classification benchmarking datasets using publicly available biomedical networks and gene annotation data. The first release version contains interfaces to networks from 15 sources and annotations from three sources.
2. We present a comprehensive benchmarking study on the OBNB node classification datasets with a wide range of graph ML approaches and tricks to set up the baseline for future comparisons.
3. We analyze the benchmarking results and point out several exciting directions and the potential need for a special class of graph neural network to tackle the OBNB tasks.

1.1 Related work

Several existing Python packages share similar goals with `obnb`, primarily focusing on establishing biomedical network datasets and facilitating their analyses. In these networks, nodes typically represent genes or their products, such as proteins, while edges represent the functional relationships between them [36], such as physical interactions. `PyGNA` [24] offers a suite of tools for analyzing and visualizing single or multiple gene sets using biological networks. `PyGenePlexus` [63] and `drug2ways` [79] specialize in network-based predictions of genes and drugs. The `OGB` [34] platform houses a variety of graph benchmarking datasets, which includes a PPI dataset akin to the STRING-GOBP dataset in OBNB (Table S11). Nonetheless, all the aforementioned packages have a limited number of, if any, biomedical network and label data. `obnb`, on the other hand, provides an extensive number of biomedical networks and diverse gene set collections to facilitate the systematic evaluation of graph machine learning methods on diverse datasets. In a related domain, `PyKEEN` [3] provides a vast array of biomedical knowledge graph (KG) datasets and KG embedding methods. There, the main task of interest is link prediction, through which the missing knowledge link can be completed. Other notable works for constructing large-scale biomedical KG and setting up link-prediction benchmarks from them include `BioCypher` [57] and `OpenBioLink` [11]. While the tasks associated with KG [95] are orthogonal to the node classification settings, it is possible to reformulate gene classification problems as KG completion and vice versa [5, 104]. Nevertheless, the advantages and drawbacks of these two approaches are yet to be comprehensively evaluated.

2 Systems description

Making the process of setting up ML-ready network biology benchmarking datasets from publicly available data as effortlessly as possible is the core mission of `obnb`. We implement and package a suite of graph (`obnb.graph`) and label (`obnb.label`) processing functionalities and couple them with the high-level data object `obnb.data` to provide a simple interface for users to download and process biological networks and label information. For example, calling `obnb.data.BioGRID("datasets")` and `obnb.data.DisGeNET("datasets")` will download, process, and save the BioGRID network and DisGeNET label data under the `datasets/` directory, which can then be loaded directly next time the functions are called. Users can compose a dataset object using the network and the label objects, along with the split (Section 2.3), which can then be used by a model trainer to train and evaluate a particular graph learning method. Alternatively, the composed dataset object can be transformed into data objects for standard GNN framework, including PyTorch Geometric (PyG) [25] and Deep Graph Library (DGL) [94].

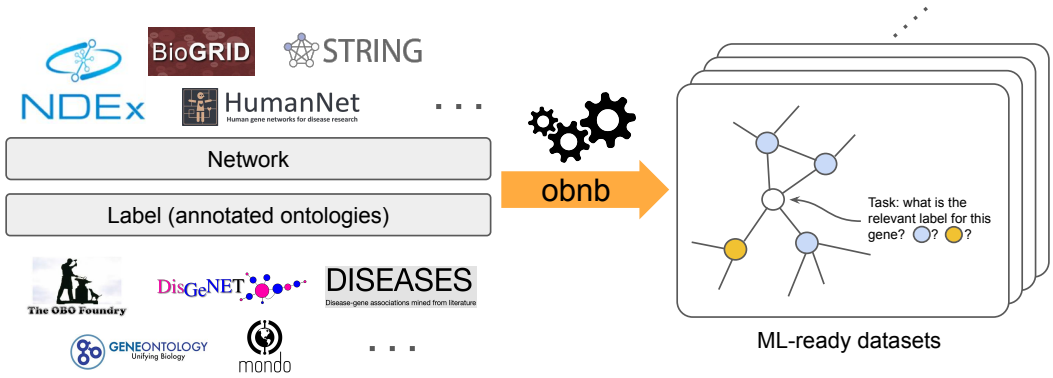

(a) `obnb` downloads network and label data from public data sources, then process and combine them into ML-ready benchmarking graph datasets.

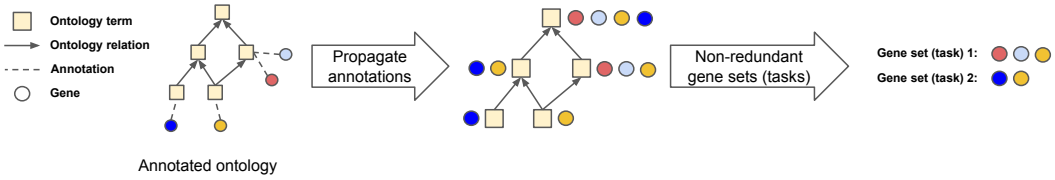

(b) Generating label data from annotated ontology through annotation propagation and non-redundant gene set extraction.

Figure 1: Overview of `obnb` data processing and benchmarking dataset generation

In the following subsections, we go into details about the processing steps for the biomedical networks (Section 2.1), creation of node labels from annotated ontologies (Section 2.2), and preparation of data splits (Section 2.3). Finally, as we are dedicated to creating a valuable resource for the community, we closely follow several open-source community standards, as elaborated in Appendix A.7.

2.1 Network

Downloading Currently, tens of genome-scale human gene interaction network databases are publicly available, each constructed and calibrated with different strategies and sources of interaction evidence [36]. Unlike in many other domains, such as chemoinformatics, where there are only a few ways to construct the graph (e.g., molecules), gene interaction networks can be defined and created in a wide range of manners, all of which capture different aspects of the functional relationships between genes. Some broad gene interaction mining strategies include experimentally captured physical protein interactions [85], gene co-expression [45], genetic interactions [19], and text-mined gene interactions [86]. We leverage the Network Data Exchange (NDEx) [78] to download the biological network data when possible (Figure 1a). The obtained `CX` stream format is then converted into a `obnb.graph` object for further processing.

Gene ID conversion In gene interaction networks, each node represents a gene or its gene product, such as a protein. There have been several standards in mapping gene identifiers, and different gene interaction networks might not use the same gene ID. For example, the STRING database [86] uses Ensembl protein ID [40], PCNet [36] uses HGNC [28], and BioGRID [85] uses Entrez gene ID [40]. Here, we use the NCBI Entrez gene ID for its advantages, such as supporting more species other than Human and being less ambiguous [33]. To convert other types of gene IDs into the Entrez gene, we use the MyGene query service [98], which provides the most up-to-date gene ID mapping across tens of gene ID types. Following, we remove any gene where more than one gene ID is mapped to the same Entrez gene, which indicates ambiguity in annotating the gene identifier currently. The gene interaction network after gene ID conversion will contain equal or less genes, all of which are one-to-one mapped from the original gene IDs to the corresponding Entrez genes.

Connected component In practice, a small fraction (typically within 1%) of genes may be disconnected from the largest connected components. The disconnectedness of the network is typically due to missing information about gene interactions from the measurement; the more information a

network uses to define the interactions, the denser and less likely there will be disconnected genes. Thus, we extract the largest connected component of the gene interaction network by default as it is more natural to have a single component for the transductive node classification tasks we consider. However, a user can also choose to take the full network without extracting the largest connected component by specifying the `largest_comp` option to `False` when initializing the data object.

2.2 Label

Many biological annotations are organized into hierarchies of abstract concepts, known as ontologies [8]. Each ontology term (a node in the ontology graph) is associated with a set of genes provided by current curated knowledge. By the hierarchical nature of the ontologies, if a gene is associated with an ontology term, then it must also be associated with any more general ontology terms. Thus, we first propagate gene annotations over the ontology, resulting in highly redundant gene set collection. Then, we pick a non-redundant subset of the gene sets with other filtering criteria to set up the final labeled data in the form of $\mathbf{Y} \in \{0,1\}^{N \times p}$ with N number of genes and p number of labels (Table 1b).

2.2.1 Annotated ontology

An ontology is a directed acyclic graph $H = (V_H, E_H)$, where $v \in V_H$ is an ontology term. The directed edge $(u, v) \in E_H$ indicates v is a parent of u, that is, v is more abstract or general concept containing u. Consider B as the set of all genes we are interested in, and $\mathcal{P}(B)$ be the power set of B. Given a gene annotation data, represented as a set of pairs $\mathcal{A} = \{(b, v)_i\}$, where $b \in B$ and $v \in V_H$ are gene and ontology term, we represent the *raw annotation* $J_0 : V_H \to \mathcal{P}(B)$ as a map from an ontology term to a set of genes, so that $J_0(v) = \{b : (b, v) \in \mathcal{A}\}$. We then propagate the *raw annotation* $J_0(\cdot)$ over the ontology H into a *propagated annotation* $J(\cdot)$, where $J(v) = \cup_{v' : \exists \text{path from} v' \text{ to } v} J_0(v')$, as depicted in Figure 1b.

Downloading All the ontology data is downloaded from the OBO Foundry [82] (Figure 1a), which actively maintains tens of large-scale biological ontologies. In the first release, we focus on three different annotations, Gene Ontology (GO) [4], DisGeNET [77], and DISEASES [30]. We naturally split GO into three different sub-collections, namely biological process (GOBP), cellular component (GOCC), and molecular function (GOMF), resulting in a total number of five label collections.

2.2.2 Filtering

The propagated annotations contain highly redundant gene sets, which may bias the benchmarking evaluations toward genes sets that commonly appear. To address this, we adapt the non-redundant gene set selection scheme used in Liu et al. [54]. In brief, we construct a graph of gene sets based on the redundancy between two gene sets, and recursively extract the most representative gene set in each connected component (Figure 1b). In addition, we provide several other filtering methods, such as filtering gene sets based on their sizes, number of occurrences, and their existence in the gene interaction network, to help further clean up the gene set collection to be used for final evaluation. Advanced users can alter these filtering functionalities to flexibly set up a custom gene set collection to better suit their biological interests besides using the default filtering steps provided by `obnb`.

2.3 Data splitting

A rigorous data splitting should closely mimic real-world scenarios to provide accurate and unbiased estimations of the models' performance. One stringent solution is temporal holdout, where the training input and label data are obtained before a specific time point, and the testing data is only available afterwards [18, 54]. In practice, this temporal setting is often too restrictive and leads to insufficient tasks for evaluation [54]. Thus, by default, we consider a closely related but less strict strategy called *study-bias holdout*.

6/2/2 study-bias holdout We use top 60% of the most studied genes with at least one associated label for training. The extend to which a gene is studied is based on its number of associated PubMed publications retrieved from NCBI. The 20% least studied genes are used for testing, and the rest of the 20% genes are used for validation. Notice that by splitting up genes this way, some of the tasks may get very few positive examples in one of the splits. Hence, we remove any task whose minimum number of positive examples across splits falls below a threshold value (set to 10 by default). For completeness, we also provide functionalities in `obnb` to generate random splits.

2.4 Dataset construction

The network (Section 2.1) and label (Section 2.2) modules provide flexible solutions for processing and setting up datasets. Meanwhile, we provide a default dataset constructor that utilizes the above modules with reasonable settings to set up a dataset given particular selections of network and label. The default dataset construction workflow is as follows.

1. Select the network and label (task collection) of interest.
2. Remove genes in the task collection that are not present in the gene interaction network.
3. Remove tasks whose number of positive examples falls below 50 after the gene filtering above.
4. Setup 6/2/2 study-bias holdout (Section 2.3).

3 Experimental settings

To provide solid baselines for future references, we benchmark a wide range of graph ML methods on our OBNB datasets. Due to space limits, we only present a subset of benchmarking results in the main paper and refer readers to Appendix C for all other results. Specifically, we only include datasets generated using the BioGRID or HumanNet network, combined with the GOBP or DisGeNET labels, resulting in four primary datasets. The two networks were chosen for their distinct characteristics: BioGRID is an unweighted graph whose edges indicate protein interaction evidence from high throughput experiments [85], whereas HumanNet is a weighted graph whose edges indicate much more diverse types of interactions such as gene coexpression and associations derived via literature text-mining [42]. Meanwhile, the two selected label collections cover two broad classes of gene classification problems, namely, gene function prediction (GOBP) and disease gene association prediction (DisGeNET). We report the performance as the average test precision over prior (APOP) score across five seeds (see Appendix A.5 for the mathematical definition and the motivation of choosing APOP as our main metric). The statistics about networks and task collections for the primary datasets are shown in Table 1 (see Table S10 and Table S11 for all dataset statistics).

Table 1: Main dataset statistics. The network density is computed as the ratio of existing edges over all possible undirected edges: $2(\#edges)/(\#nodes \times (\#nodes - 1))$.

(a) Network statistics

	# nodes	# edges	Density
BioGRID	18,951	1,103,298	0.0030
HumanNet	17,211	847,104	0.0029

(b) Label set collection statistics

	# tasks	# positives
DisGeNET	298	198.6 ± 135.0
GOBP	105	88.4 ± 35.3

3.1 Baselines

We consider three general types of methods: (1) label propagation [105] that directly propagates label information over the graph, (2) graph embedding that first extracts the vectorial representations of each node in the graph, which are then used to fit a simple classifier, such as logistic regression, and (3) GNN that learns the mapping from each node to its label space end-to-end. All implementation details, including technical descriptions of the featurization, the backbone graph neural network architecture, and hyperparameter settings, can be found in the Appendix A.

Graph embeddings We include three distinct featurizations in the main result: using the rows of the adjacency matrix as the node features (Adj) [54], using the *node2vec* embedding (N2V) [31], or using the Laplacian EigenMap embedding (LapEigMap) [9]. Extended results using SVD, LINE [87], and Walklets [75] are available in the Appendix (Table S6). Each of these features is coupled with an ℓ_2 regularized logistic regression model (LogReg) for downstream prediction.

GNN We include multiple variations of two GNN, GCN [48] and GAT [90], in the main results. Extended results for SAGE [32], GIN [102], and GatedGCN [12] can be found in the Appendix (Table S6). One major challenge in applying GNN to OBNB datasets is the lack of canonical node features. This is unlike networks in other domains, such as citation networks, where node features are naturally defined using the paper content, such as bag of words [34]. To tackle this problem, we experiment with a diverse selection of node featurization strategies, including using the one hot

Table 2: Performance of different methods on the four primary OBNB datasets evaluated in APOP ↑ aggregated over five seeds. **Bold** indicates the best-performing method within the method class (traditional ML or GNN). Green indicates best performing-method across both classes. See Table S7 for extended baseline performance references.

			BioGRID		HumanNet	
Model	Features	C&S?	DisGeNET	GOBP	DisGeNET	GOBP
LabelProp	–	✗	**0.931 ± 0.000**	1.885 ± 0.000	**3.059 ± 0.000**	3.806 ± 0.000
LogReg	Adj	✗	0.743 ± 0.000	2.528 ± 0.000	3.053 ± 0.000	3.964 ± 0.006
LogReg	N2V	✗	0.836 ± 0.029	**2.571 ± 0.015**	2.433 ± 0.029	**4.036 ± 0.019**
LogReg	LapEigMap	✗	0.864 ± 0.002	2.149 ± 0.000	2.301 ± 0.000	3.778 ± 0.001
GCN	LogDeg	✗	0.773 ± 0.035	2.022 ± 0.100	2.452 ± 0.107	3.524 ± 0.061
GCN	LogDeg	✓	1.026 ± 0.013	2.201 ± 0.035	2.777 ± 0.031	3.743 ± 0.015
GCN†	N2V+LogDeg+Label	✓	1.014 ± 0.020	2.411 ± 0.044	3.053 ± 0.078	3.921 ± 0.045
GCN‡	N2V+LogDeg+Label	✓	1.012 ± 0.040	2.572 ± 0.066	**3.116 ± 0.017**	3.812 ± 0.071
GAT	LogDeg	✗	0.552 ± 0.111	1.592 ± 0.408	2.547 ± 0.207	3.571 ± 0.159
GAT	LogDeg	✓	1.002 ± 0.018	2.227 ± 0.024	3.007 ± 0.037	3.876 ± 0.053
GAT†	N2V+LogDeg+Label	✓	1.037 ± 0.036	**2.624 ± 0.070**	3.100 ± 0.031	3.908 ± 0.086
GAT‡	N2V+LogDeg+Label	✓	**1.063 ± 0.023**	2.562 ± 0.070	3.065 ± 0.021	**3.963 ± 0.082**

† recommended BoT, ‡ recommended BoT with fully tuned GNNs (see Appendix A.4.1 for tuning details)

encoded log degree of the node, using *node2vec*, and many others. We provide detailed descriptions for the 15 different feature construction strategies in Appendix A.3.1, with extended results for GCN and GAT in Table S5.

Bag of Tricks (BoT) In addition to optimizing the model architectures, many tricks in model training and feature augmentations have also shown to be key factors for practically good performance in existing benchmarks [34]. Here, we further investigate the usefulness of several popular tricks, including reusing training labels as node features (LabelReuse) [97] and performing post-correction to the predictions at test time via correct and smooth (C&S) [39].

4 Results and discussions

4.1 Traditional ML methods perform comparably to GNNs overall

Table 2 shows the overall performance for the selected model on the four primary benchmarking datasets (full baseline results in Table S6). Surprisingly, even after a rather extensive hyperparameter search and GNN architecture tuning (Appendix A.4), logistic regression using graph-derived features still performs comparably to GNNs. For example, *node2vec* achieves the best performance for GOBP prediction when using both BioGRID and HumanNet. Similar results are obtained when using the other networks (Table S6) and using the more standard random splitting strategy (Table S8). The superior performance of traditional ML methods over GNNs is in stark contrast with results reported in recent benchmarking studies [81, 23, 34], highlighting the unique characteristics of biological networks and the challenges in modeling them. In addition, we demonstrate that the proposed study-bias holdout splitting provides more stringent evaluations than random splitting (Table S8).

Recommendation of BoT for GNNs While plain GNNs without BoT yield relatively unsatisfactory performances, carefully crafted BoT can bring significant enhancement to GNNs in our benchmark. First, a systematic benchmark on GCN and GAT with 15 different feature construction reveals that using *node2vec* as node features consistently achieve top performance across datasets (Figure S2). Second, reusing training labels as features also elevates overall performance, most notably for GAT (Figure S3). Third, C&S post-processing universally improves performance for both GNN and logistic regression methods, with, on average, 0.27 improvement in test APOP scores (Figure S3,S4). In light of these observations, we recommend an optimized BoT as follows: (1) use a combination of LogDeg encodings, *node2vec* embeddings, and training labels as input node features, (2) apply C&S post-

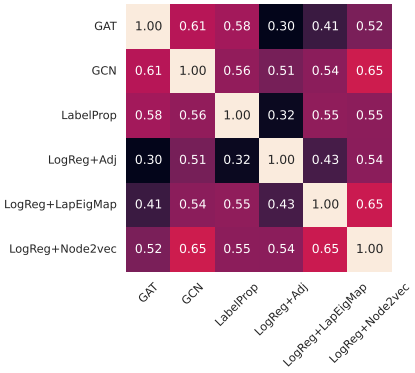

Figure 2: Correlations between methods across tasks in BioGRID-DisGeNET.

processing to refine predictions further. Our results indicate that the recommended BoT helps improve GNNs' performances by 0.36 APOP test scores on average across datasets.

4.2 Different models have their own strength

Despite the overall rankings of different methods indicating the superiority of their gene classification capabilities, no single method can achieve the best results across all tasks. We demonstrate this in Figure 2, which shows that the performance of most methods does not correlate with each other across different tasks on the BioGRID-DisGeNET dataset. For example, while LogReg+Adj performs better than GAT+LogDeg overall on the BioGRID-DisGeNET dataset, GAT+LogDeg achieves significantly better predictions (t-test p-value < 0.01) for a handful of tasks (Appendix S9), such as iris disorder and ocular vascular disorder.

Focusing on the optimal model for one or a few tasks of interest is utterly essential. This is because, in practice, experimental biologists often come with only one or a few gene sets and want to either obtain new related genes or reprioritize them based on their relevance to the whole gene set [62]. Therefore, understanding the characteristics of the task that for which a particular model works well over others is the key to making better architectural decisions for a new task of interest and, ultimately, designing new specialized GNN for network biology.

4.3 Homophily is a driving factor for good predictions

Homophily describes the tendency of a node's neighborhood to have similar labels to itself. Such effects are prevalent in many real-world graphs, such as citation networks, and have been studied extensively recently in the GNN communities as a way to understand *what* information can or cannot be captured by GNN effectively [59, 61]. Intuitively, homophily aligns well with the *guilt-by-association* principle in network biology, which similarly states that genes that interact with each other are likely functionally related. Despite this clear connection, existing homophily measures, such as the homophily ratio [61], do not straightforwardly apply to the OBNB datasets for two reasons.

1. Most established work on homophily consider *multiclass* classification task, where each node has exactly one class label, contrasting with the *multilabel* classification tasks in OBNB.
2. Label information in OBNB datasets is incredibly sparse. On average, there are only hundreds of positive genes per class out of the total number of 20K genes.

One attempt to resolve the first issue is to compute the average homophily ratio for each class independently. However, due to the label scarcity, the resulting metric can not be readily interpreted. In particular, the highest homophily ratio observed in our main benchmarking study is about 0.2 (Figure 3). Datasets with this value are typically categorized into heterophily (not homophily), contradicting the guilt-by-association principle. To address this inconsistency, we propose a corrected version of the homophily ratio that takes label scarcity into account (see Appendix A.6). The main idea is to measure homophily as a relative measurement: *how much more likely nodes labeled in class i are connected with nodes also labeled in class i than those not in class i*? This measure is directly interpretable as it is the log fold change of the homophily between positive and negative examples.

Corrected homophily ratio characterizes prediction performance of graph ML methods As shown in the right two panels of Figure 3, the corrected homophily ratio is well correlated with the prediction performance across different networks and tasks. This positive correlation unveils the fundamental principle that graph ML methods rely on: the underlying graph must provide sufficient contrast between the neighborhoods of the positive and negative examples. Conversely, the left two panels of Figure 3 indicate that the standard homophily ratio fails to adequately account for the performance nuances in low homophily tasks As a result, OBNB opens up new research opportunities in understanding the effects of homophily in GNN by introducing a new type of homophily that differs significantly from those traditionally studied [61].

Graph based augmentation tricks offer most advantages on intermediate homophilic tasks We next investigate the relationship between the corrected homophily ratio and the performance difference between a pair of methods by asking: *is one method systematically better than another method on a particular range of homophily?* The first and second rows of Figure S5 indicate that GNN augmented with different grpah-based tricks, such as C&S and *node2vec* features, provide most apparent advantage at intermediate homophily (corrected homophily ratio of ~ 2.5). However, as the homophily increases further, the performance differences diminish, suggesting that all methods would perform equally perfectly as the graph provide more clear clues about the labels. Similar trends

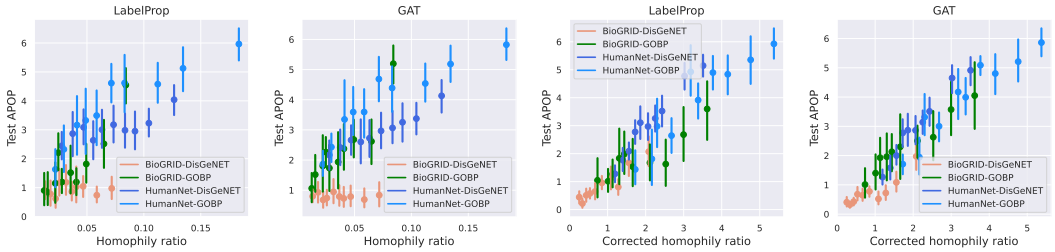

Figure 3: Relationship between the (corrected) homophily ratios of tasks and their performances.

are observed for the comparison between GAT+BoT and baseline label propagation and logistic regression methods (Figure S5 third row), where GAT+BoT most significantly outperforms the baselines at intermediate homophily.

4.4 Challenges for the OBNB benchmarks and potential future directions

Our systematic benchmarking study paves the way for numerous subsequent explorations. Below, we outline the primary challenges associated with OBNB and suggest potential areas for future research.

Challenge 1. Lack of canonical node features Traditional network biology studies solely rely on biological network structures to gain insights [7, 6, 49]. Meanwhile, the presence of rich node features in many existing graph benchmarks is crucial for the success of GNNs [55], posing a challenge for GNNs in learning without meaningful node features. An exciting and promising future direction for obtaining meaningful node features is by leveraging the sequential or structural information of the gene product (e.g., protein) using large-scale biological pre-trained language models like ESM-2 [53].

Challenge 2. Dense and weighted graphs Many gene interaction networks are dense and weighted by construction, such as coexpression [45] or integrated functional interactions [86]. In more extreme cases, the weighted networks can be fully connected [29]. The networks used in the OBNB benchmark are orders of magnitude denser than citation networks [81] (Table 1a). Thus, scalably and effectively learning from densely weighted gene interaction networks is an area of research to be further explored in the future [56]. One potential solution would be first sparsifying the original dense network before proceeding to train GNN models on them, either by straightforwardly applying an edge cutoff threshold or by using more intricated methods such as spectral sparsification [84].

Challenge 3. Scarce labeled data Curated biological annotations are scarce, posing the challenge of effectively training powerful and expressive models with limited labeled examples. Furthermore, a particular gene can be labeled with more than one biological annotation (multi-label setting), which is much more complex than the multi-class settings in popular benchmarking graph datasets such as Cora and CiteSeer [81]. The data scarcity issue naturally invites the usage of self-supervised [101] graph learning techniques, such as DGI [91], and knowledge transfer via pre-training, such as TxGNN [38]. However, these methods still face the challenge of missing node features (challenge 1).

Challenge 4. Low corrected homophily ratio tasks Our results in Figure 3 show that tasks with low corrected homophily ratios tend to be more challenging to predict, indicating that current tested methods are limited to local information of the underlying graph. This naturally opens up opportunities for designing models that (1) better capture long-range dependencies [22] and (2) exploit higher-order structural information [65].

5 Conclusion

We have developed `obnb`, an open-source Python package for rapidly setting up ML-ready benchmarking graph datasets using diverse biomedical networks and gene annotations from publicly available sources. `obnb` takes care of tedious data (pre-)processing steps so that network biologists can easily set up particular datasets with their desired settings, and graph ML researchers can directly use the ML-ready datasets for model development. We have established a comprehensive set of baseline performances on OBNB using a wide range of graph ML methods for future reference and pointed out potential improvements that could further enhance performances. Together, OBNB will help accelerate the development of advanced graph ML methods in network biology toward furthering our understanding of the complex genetic basis of human traits and diseases.

Acknowledgments and Disclosure of Funding

Funding: This work was supported by NIH NIGMS R35 GM12876 to AK.

Competing interest: The authors declare no competing interests.

References

[1] Gregorio Alanis-Lobato, Miguel A Andrade-Navarro, and Martin H Schaefer. Hippie v2. 0: enhancing meaningfulness and reliability of protein–protein interaction networks. *Nucleic acids research*, page gkw985, 2016.

[2] Réka Albert. Scale-free networks in cell biology. *Journal of cell science*, 118(21):4947–4957, 2005.

[3] Mehdi Ali, Max Berrendorf, Charles Tapley Hoyt, Laurent Vermue, Sahand Sharifzadeh, Volker Tresp, and Jens Lehmann. Pykeen 1.0: A python library for training and evaluating knowledge graph embeddings. *J. Mach. Learn. Res.*, 22(82):1–6, 2021.

[4] Michael Ashburner, Catherine A Ball, Judith A Blake, David Botstein, Heather Butler, J Michael Cherry, Allan P Davis, Kara Dolinski, Selina S Dwight, Janan T Eppig, et al. Gene ontology: tool for the unification of biology. *Nature genetics*, 25(1):25–29, 2000.

[5] Sezin Kircali Ata, Min Wu, Yuan Fang, Le Ou-Yang, Chee Keong Kwoh, and Xiao-Li Li. Recent advances in network-based methods for disease gene prediction. *Briefings in bioinformatics*, 22(4):bbaa303, 2021.

[6] Albert-Laszlo Barabasi and Zoltan N Oltvai. Network biology: understanding the cell's functional organization. *Nature reviews genetics*, 5(2):101–113, 2004.

[7] Albert-László Barabási, Natali Gulbahce, and Joseph Loscalzo. Network medicine: a network-based approach to human disease. *Nature reviews genetics*, 12(1):56–68, 2011.

[8] Jonathan BL Bard and Seung Y Rhee. Ontologies in biology: design, applications and future challenges. *nature reviews genetics*, 5(3):213–222, 2004.

[9] Mikhail Belkin and Partha Niyogi. Laplacian eigenmaps for dimensionality reduction and data representation. *Neural computation*, 15(6):1373–1396, 2003.

[10] Lukas Biewald. Experiment tracking with weights and biases, 2020. URL https://www.wandb.com/. Software available from wandb.com.

[11] Anna Breit, Simon Ott, Asan Agibetov, and Matthias Samwald. Openbiolink: a benchmarking framework for large-scale biomedical link prediction. *Bioinformatics*, 36(13):4097–4098, 2020.

[12] Xavier Bresson and Thomas Laurent. Residual gated graph convnets. *arXiv preprint arXiv:1711.07553*, 2017.

[13] Shaked Brody, Uri Alon, and Eran Yahav. How attentive are graph attention networks? In *International Conference on Learning Representations*, 2021.

[14] Hongyun Cai, Vincent W Zheng, and Kevin Chen-Chuan Chang. A comprehensive survey of graph embedding: Problems, techniques, and applications. *IEEE Transactions on Knowledge and Data Engineering*, 30(9):1616–1637, 2018.

[15] Luca Cappelletti, Tommaso Fontana, Elena Casiraghi, Vida Ravanmehr, Tiffany J. Callahan, Carlos Cano, Marcin P. Joachimiak, Christopher J. Mungall, Peter N. Robinson, Justin Reese, and Giorgio Valentini. GRAPE for fast and scalable graph processing and random-walk-based embedding. *Nature Computational Science*, 3(6):552–568, June 2023. doi: 10.1038/s43588-023-00465-8.

[16] Lenore Cowen, Trey Ideker, Benjamin J Raphael, and Roded Sharan. Network propagation: a universal amplifier of genetic associations. *Nature Reviews Genetics*, 18(9):551–562, 2017.

[17] Hejie Cui, Zijie Lu, Pan Li, and Carl Yang. On positional and structural node features for graph neural networks on non-attributed graphs. In *Proceedings of the 31st ACM International Conference on Information & Knowledge Management*, pages 3898–3902, 2022.

[18] Christophe Dessimoz, Nives Škunca, and Paul D Thomas. Cafa and the open world of protein function predictions. *Trends in Genetics*, 29(11):609–610, 2013.

[19] Scott J Dixon, Michael Costanzo, Anastasia Baryshnikova, Brenda Andrews, Charles Boone, et al. Systematic mapping of genetic interaction networks. *Annual review of genetics*, 43(1): 601–625, 2009.

[20] Kevin Drew, John B Wallingford, and Edward M Marcotte. hu. map 2.0: integration of over 15,000 proteomic experiments builds a global compendium of human multiprotein assemblies. *Molecular Systems Biology*, 17(5):e10016, 2021.

[21] Vijay Prakash Dwivedi, Anh Tuan Luu, Thomas Laurent, Yoshua Bengio, and Xavier Bresson. Graph neural networks with learnable structural and positional representations. In *International Conference on Learning Representations*, 2021.

[22] Vijay Prakash Dwivedi, Ladislav Rampášek, Michael Galkin, Ali Parviz, Guy Wolf, Anh Tuan Luu, and Dominique Beaini. Long range graph benchmark. *Advances in Neural Information Processing Systems*, pages 22326–22340, 2022.

[23] Vijay Prakash Dwivedi, Chaitanya K Joshi, Anh Tuan Luu, Thomas Laurent, Yoshua Bengio, and Xavier Bresson. Benchmarking graph neural networks. *Journal of Machine Learning Research*, 24(43):1–48, 2023.

[24] Viola Fanfani, Fabio Cassano, and Giovanni Stracquadanio. Pygna: a unified framework for geneset network analysis. *BMC bioinformatics*, 21(1):1–22, 2020.

[25] Matthias Fey and Jan Eric Lenssen. Fast graph representation learning with pytorch geometric. In *ICLR workshop on representation learning on graphs and manifolds*, 2019.

[26] Justin Gilmer, Samuel S Schoenholz, Patrick F Riley, Oriol Vinyals, and George E Dahl. Neural message passing for quantum chemistry. In *International conference on machine learning*, pages 1263–1272. PMLR, 2017.

[27] Palash Goyal and Emilio Ferrara. Graph embedding techniques, applications, and performance: A survey. *Knowledge-Based Systems*, 151:78–94, 2018.

[28] Kristian A Gray, Bethan Yates, Ruth L Seal, Mathew W Wright, and Elspeth A Bruford. Genenames. org: the hgnc resources in 2015. *Nucleic acids research*, 43(D1):D1079–D1085, 2015.

[29] Casey S Greene, Arjun Krishnan, Aaron K Wong, Emanuela Ricciotti, Rene A Zelaya, Daniel S Himmelstein, Ran Zhang, Boris M Hartmann, Elena Zaslavsky, Stuart C Sealfon, et al. Understanding multicellular function and disease with human tissue-specific networks. *Nature genetics*, 47(6):569–576, 2015.

[30] Dhouha Grissa, Alexander Junge, Tudor I Oprea, and Lars Juhl Jensen. Diseases 2.0: a weekly updated database of disease–gene associations from text mining and data integration. *Database*, 2022, 2022.

[31] Aditya Grover and Jure Leskovec. node2vec: Scalable feature learning for networks. In *Proceedings of the 22nd ACM SIGKDD international conference on Knowledge discovery and data mining*, pages 855–864, 2016.

[32] Will Hamilton, Zhitao Ying, and Jure Leskovec. Inductive representation learning on large graphs. *Advances in neural information processing systems*, 30, 2017.

[33] Daniel Himmelstein, Casey Greene, and Alexander Pico. Using entrez gene as our gene vocabulary, February 2015. URL https://doi.org/10.15363/thinklab.d34.

[34] Weihua Hu, Matthias Fey, Marinka Zitnik, Yuxiao Dong, Hongyu Ren, Bowen Liu, Michele Catasta, and Jure Leskovec. Open graph benchmark: Datasets for machine learning on graphs. *Advances in neural information processing systems*, 33:22118–22133, 2020.

[35] Weihua Hu, Matthias Fey, Hongyu Ren, Maho Nakata, Yuxiao Dong, and Jure Leskovec. Ogb-lsc: A large-scale challenge for machine learning on graphs. In *Thirty-fifth Conference on Neural Information Processing Systems Datasets and Benchmarks Track (Round 2)*, 2021.

[36] Justin K Huang, Daniel E Carlin, Michael Ku Yu, Wei Zhang, Jason F Kreisberg, Pablo Tamayo, and Trey Ideker. Systematic evaluation of molecular networks for discovery of disease genes. *Cell systems*, 6(4):484–495, 2018.

[37] Kexin Huang, Tianfan Fu, Wenhao Gao, Yue Zhao, Yusuf Roohani, Jure Leskovec, Connor Coley, Cao Xiao, Jimeng Sun, and Marinka Zitnik. Therapeutics data commons: Machine learning datasets and tasks for drug discovery and development. *Advances in neural information processing systems*, 2021.

[38] Kexin Huang, Payal Chandak, Qianwen Wang, Shreyas Havaldar, Akhil Vaid, Jure Leskovec, Girish Nadkarni, Benjamin S Glicksberg, Nils Gehlenborg, and Marinka Zitnik. Zero-shot prediction of therapeutic use with geometric deep learning and clinician centered design. *medRxiv*, pages 2023–03, 2023.

[39] Qian Huang, Horace He, Abhay Singh, Ser-Nam Lim, and Austin Benson. Combining label propagation and simple models out-performs graph neural networks. In *International Conference on Learning Representations*, 2020.

[40] T Hubbard, D Andrews, Mario Cáccamo, Graham Cameron, Yuan Chen, M Clamp, Laura Clarke, Guy Coates, Tony Cox, Fiona Cunningham, et al. Ensembl 2005. *Nucleic acids research*, 33(suppl_1):D447–D453, 2005.

[41] Edward L Huttlin, Raphael J Bruckner, Jose Navarrete-Perea, Joe R Cannon, Kurt Baltier, Fana Gebreab, Melanie P Gygi, Alexandra Thornock, Gabriela Zarraga, Stanley Tam, et al. Dual proteome-scale networks reveal cell-specific remodeling of the human interactome. *Cell*, 184(11):3022–3040, 2021.

[42] Sohyun Hwang, Chan Yeong Kim, Sunmo Yang, Eiru Kim, Traver Hart, Edward M Marcotte, and Insuk Lee. Humannet v2: human gene networks for disease research. *Nucleic acids research*, 47(D1):D573–D580, 2019.

[43] Trey Ideker and Roded Sharan. Protein networks in disease. *Genome research*, 18(4):644–652, 2008.

[44] Junzhong Ji, Aidong Zhang, Chunnian Liu, Xiaomei Quan, and Zhijun Liu. Survey: Functional module detection from protein-protein interaction networks. *IEEE Transactions on Knowledge and Data Engineering*, 26(2):261–277, 2012.

[45] Kayla A Johnson and Arjun Krishnan. Robust normalization and transformation techniques for constructing gene coexpression networks from rna-seq data. *Genome biology*, 23(1):1–26, 2022.

[46] Atanas Kamburov, Konstantin Pentchev, Hanna Galicka, Christoph Wierling, Hans Lehrach, and Ralf Herwig. Consensuspathdb: toward a more complete picture of cell biology. *Nucleic acids research*, 39(suppl_1):D712–D717, 2011.

[47] Minoru Kanehisa. The kegg database. In *'In Silico'Simulation of Biological Processes: Novartis Foundation Symposium 247*, volume 247, pages 91–103. Wiley Online Library, 2002.

[48] Thomas N Kipf and Max Welling. Semi-supervised classification with graph convolutional networks. In *International Conference on Learning Representations*, 2016.

[49] Sebastian Köhler, Sebastian Bauer, Denise Horn, and Peter N Robinson. Walking the interactome for prioritization of candidate disease genes. *The American Journal of Human Genetics*, 82(4):949–958, 2008.

[50] Georg Kustatscher, Piotr Grabowski, Tina A Schrader, Josiah B Passmore, Michael Schrader, and Juri Rappsilber. Co-regulation map of the human proteome enables identification of protein functions. *Nature biotechnology*, 37(11):1361–1371, 2019.

[51] Insuk Lee, U Martin Blom, Peggy I Wang, Jung Eun Shim, and Edward M Marcotte. Prioritizing candidate disease genes by network-based boosting of genome-wide association data. *Genome research*, 21(7):1109–1121, 2011.

[52] Pan Li, Yanbang Wang, Hongwei Wang, and Jure Leskovec. Distance encoding: Design provably more powerful neural networks for graph representation learning. *Advances in Neural Information Processing Systems*, 33:4465–4478, 2020.

[53] Zeming Lin, Halil Akin, Roshan Rao, Brian Hie, Zhongkai Zhu, Wenting Lu, Nikita Smetanin, Robert Verkuil, Ori Kabeli, Yaniv Shmueli, et al. Evolutionary-scale prediction of atomic-level protein structure with a language model. *Science*, 379(6637):1123–1130, 2023.

[54] Renming Liu, Christopher A Mancuso, Anna Yannakopoulos, Kayla A Johnson, and Arjun Krishnan. Supervised learning is an accurate method for network-based gene classification. *Bioinformatics*, 36(11):3457–3465, 2020.

[55] Renming Liu, Semih Cantürk, Frederik Wenkel, Sarah McGuire, Xinyi Wang, Anna Little, Leslie O'Bray, Michael Perlmutter, Bastian Rieck, Matthew Hirn, et al. Taxonomy of benchmarks in graph representation learning. In *Learning on Graphs Conference*, pages 6–1. PMLR, 2022.

[56] Renming Liu, Matthew Hirn, and Arjun Krishnan. Accurately modeling biased random walks on weighted networks using node2vec+. *Bioinformatics*, 39(1):btad047, 2023.

[57] Sebastian Lobentanzer, Patrick Aloy, Jan Baumbach, Balazs Bohar, Vincent J Carey, Pornpimol Charoentong, Katharina Danhauser, Tunca Doğan, Johann Dreo, Ian Dunham, et al. Democratizing knowledge representation with biocypher. *Nature Biotechnology*, pages 1–4, 2023.

[58] Ilya Loshchilov and Frank Hutter. Decoupled weight decay regularization. In *International Conference on Learning Representations*, 2018.

[59] Sitao Luan, Chenqing Hua, Qincheng Lu, Jiaqi Zhu, Mingde Zhao, Shuyuan Zhang, Xiao-Wen Chang, and Doina Precup. Is heterophily a real nightmare for graph neural networks to do node classification? *arXiv preprint arXiv:2109.05641*, 2021.

[60] Katja Luck, Dae-Kyum Kim, Luke Lambourne, Kerstin Spirohn, Bridget E Begg, Wenting Bian, Ruth Brignall, Tiziana Cafarelli, Francisco J Campos-Laborie, Benoit Charloteaux, et al. A reference map of the human binary protein interactome. *Nature*, 580(7803):402–408, 2020.

[61] Yao Ma, Xiaorui Liu, Neil Shah, and Jiliang Tang. Is homophily a necessity for graph neural networks? In *International Conference on Learning Representations*, 2021.

[62] Christopher A Mancuso, Patrick S Bills, Douglas Krum, Jacob Newsted, Renming Liu, and Arjun Krishnan. Geneplexus: a web-server for gene discovery using network-based machine learning. *Nucleic Acids Research*, 2022.

[63] Christopher A Mancuso, Renming Liu, and Arjun Krishnan. Pygeneplexus: A python package for gene discovery using network-based machine learning. *bioRxiv*, 2022.

[64] Tomas Mikolov, Ilya Sutskever, Kai Chen, Greg S Corrado, and Jeff Dean. Distributed representations of words and phrases and their compositionality. *Advances in neural information processing systems*, 26, 2013.

[65] Christopher Morris, Martin Ritzert, Matthias Fey, William L Hamilton, Jan Eric Lenssen, Gaurav Rattan, and Martin Grohe. Weisfeiler and leman go neural: Higher-order graph neural networks. In *Proceedings of the AAAI conference on artificial intelligence*, pages 4602–4609, 2019.

[66] Sara Mostafavi, Debajyoti Ray, David Warde-Farley, Chris Grouios, and Quaid Morris. Genemania: a real-time multiple association network integration algorithm for predicting gene function. *Genome biology*, 9:1–15, 2008.

[67] Giulia Muzio, Leslie O'Bray, and Karsten Borgwardt. Biological network analysis with deep learning. *Briefings in bioinformatics*, 22(2):1515–1530, 2021.

[68] Walter Nelson, Marinka Zitnik, Bo Wang, Jure Leskovec, Anna Goldenberg, and Roded Sharan. To embed or not: network embedding as a paradigm in computational biology. *Frontiers in genetics*, 10:381, 2019.

[69] Stephen Oliver. Guilt-by-association goes global. *Nature*, 403(6770):601–602, 2000.

[70] Adam Paszke, Sam Gross, Francisco Massa, Adam Lerer, James Bradbury, Gregory Chanan, Trevor Killeen, Zeming Lin, Natalia Gimelshein, Luca Antiga, et al. Pytorch: An imperative style, high-performance deep learning library. *Advances in neural information processing systems*, 32, 2019.

[71] Fabian Pedregosa, Gaël Varoquaux, Alexandre Gramfort, Vincent Michel, Bertrand Thirion, Olivier Grisel, Mathieu Blondel, Peter Prettenhofer, Ron Weiss, Vincent Dubourg, et al. Scikit-learn: Machine learning in python. *the Journal of machine Learning research*, 12:2825–2830, 2011.

[72] Hongbin Pei, Bingzhe Wei, Kevin Chen-Chuan Chang, Yu Lei, and Bo Yang. Geom-gcn: Geometric graph convolutional networks. In *International Conference on Learning Representations*, 2019.

[73] Livia Perfetto, Leonardo Briganti, Alberto Calderone, Andrea Cerquone Perpetuini, Marta Iannuccelli, Francesca Langone, Luana Licata, Milica Marinkovic, Anna Mattioni, Theodora Pavlidou, et al. Signor: a database of causal relationships between biological entities. *Nucleic acids research*, 44(D1):D548–D554, 2016.

[74] Bryan Perozzi, Rami Al-Rfou, and Steven Skiena. Deepwalk: Online learning of social representations. In *Proceedings of the 20th ACM SIGKDD international conference on Knowledge discovery and data mining*, pages 701–710, 2014.

[75] Bryan Perozzi, Vivek Kulkarni, Haochen Chen, and Steven Skiena. Don't walk, skip! online learning of multi-scale network embeddings. In *Proceedings of the 2017 IEEE/ACM International Conference on Advances in Social Networks Analysis and Mining 2017*, pages 258–265, 2017.

[76] Emma Persson, Miguel Castresana-Aguirre, Davide Buzzao, Dimitri Guala, and Erik LL Sonnhammer. Funcoup 5: functional association networks in all domains of life, supporting directed links and tissue-specificity. *Journal of Molecular Biology*, 433(11):166835, 2021.

[77] Janet Piñero, Àlex Bravo, Núria Queralt-Rosinach, Alba Gutiérrez-Sacristán, Jordi Deu-Pons, Emilio Centeno, Javier García-García, Ferran Sanz, and Laura I Furlong. Disgenet: a comprehensive platform integrating information on human disease-associated genes and variants. *Nucleic acids research*, page gkw943, 2016.

[78] Dexter Pratt, Jing Chen, David Welker, Ricardo Rivas, Rudolf Pillich, Vladimir Rynkov, Keiichiro Ono, Carol Miello, Lyndon Hicks, Sandor Szalma, et al. Ndex, the network data exchange. *Cell systems*, 1(4):302–305, 2015.

[79] Daniel Rivas-Barragan, Sarah Mubeen, Francesc Guim Bernat, Martin Hofmann-Apitius, and Daniel Domingo-Fernández. Drug2ways: Reasoning over causal paths in biological networks for drug discovery. *PLoS computational biology*, 16(12):e1008464, 2020.

[80] Takaya Saito and Marc Rehmsmeier. The precision-recall plot is more informative than the roc plot when evaluating binary classifiers on imbalanced datasets. *PloS one*, 10(3):e0118432, 2015.

[81] Oleksandr Shchur, Maximilian Mumme, Aleksandar Bojchevski, and Stephan Günnemann. Pitfalls of graph neural network evaluation. *Relational Representation Learning Workshop, NeurIPS 2018*, 2018.

[82] Barry Smith, Michael Ashburner, Cornelius Rosse, Jonathan Bard, William Bug, Werner Ceusters, Louis J Goldberg, Karen Eilbeck, Amelia Ireland, Christopher J Mungall, et al. The obo foundry: coordinated evolution of ontologies to support biomedical data integration. *Nature biotechnology*, 25(11):1251–1255, 2007.

[83] Helen R Sofaer, Jennifer A Hoeting, and Catherine S Jarnevich. The area under the precision-recall curve as a performance metric for rare binary events. *Methods in Ecology and Evolution*, 10(4):565–577, 2019.

[84] Daniel A Spielman and Shang-Hua Teng. Spectral sparsification of graphs. *SIAM Journal on Computing*, 40(4):981–1025, 2011.

[85] Chris Stark, Bobby-Joe Breitkreutz, Teresa Reguly, Lorrie Boucher, Ashton Breitkreutz, and Mike Tyers. Biogrid: a general repository for interaction datasets. *Nucleic acids research*, 34 (suppl_1):D535–D539, 2006.

[86] Damian Szklarczyk, Annika L Gable, David Lyon, Alexander Junge, Stefan Wyder, Jaime Huerta-Cepas, Milan Simonovic, Nadezhda T Doncheva, John H Morris, Peer Bork, et al. String v11: protein–protein association networks with increased coverage, supporting functional discovery in genome-wide experimental datasets. *Nucleic acids research*, 47(D1): D607–D613, 2019.

[87] Jian Tang, Meng Qu, Mingzhe Wang, Ming Zhang, Jun Yan, and Qiaozhu Mei. Line: Large-scale information network embedding. In *Proceedings of the 24th international conference on world wide web*, pages 1067–1077, 2015.

[88] Dénes Türei, Tamás Korcsmáros, and Julio Saez-Rodriguez. Omnipath: guidelines and gateway for literature-curated signaling pathway resources. *Nature methods*, 13(12):966–967, 2016.

[89] Nicole A Vasilevsky, Nicolas A Matentzoglu, Sabrina Toro, Joseph E Flack IV, Harshad Hegde, Deepak R Unni, Gioconda F Alyea, Joanna S Amberger, Larry Babb, James P Balhoff, et al. Mondo: Unifying diseases for the world, by the world. *medRxiv*, pages 2022–04, 2022.

[90] Petar Veličković, Guillem Cucurull, Arantxa Casanova, Adriana Romero, Pietro Liò, and Yoshua Bengio. Graph attention networks. In *International Conference on Learning Representations*, 2018.

[91] Petar Velickovic, William Fedus, William L Hamilton, Pietro Liò, Yoshua Bengio, and R Devon Hjelm. Deep graph infomax. *ICLR (Poster)*, 2(3):4, 2019.

[92] Daniel V Veres, Dávid M Gyurkó, Benedek Thaler, Kristof Z Szalay, Dávid Fazekas, Tamás Korcsmáros, and Peter Csermely. Comppi: a cellular compartment-specific database for protein–protein interaction network analysis. *Nucleic acids research*, 43(D1):D485–D493, 2015.

[93] Marc Vidal, Michael E Cusick, and Albert-László Barabási. Interactome networks and human disease. *Cell*, 144(6):986–998, 2011.

[94] Minjie Yu Wang. Deep graph library: Towards efficient and scalable deep learning on graphs. In *ICLR workshop on representation learning on graphs and manifolds*, 2019.

[95] Quan Wang, Zhendong Mao, Bin Wang, and Li Guo. Knowledge graph embedding: A survey of approaches and applications. *IEEE Transactions on Knowledge and Data Engineering*, 29 (12):2724–2743, 2017.

[96] Xiujuan Wang, Natali Gulbahce, and Haiyuan Yu. Network-based methods for human disease gene prediction. *Briefings in functional genomics*, 10(5):280–293, 2011.

[97] Yangkun Wang, Jiarui Jin, Weinan Zhang, Yong Yu, Zheng Zhang, and David Wipf. Bag of tricks for node classification with graph neural networks. *arXiv preprint arXiv:2103.13355*, 2021.

[98] Chunlei Wu, Adam Mark, and Andrew I Su. Mygene. info: gene annotation query as a service. *bioRxiv*, page 009332, 2014.

[99] Zhenqin Wu, Bharath Ramsundar, Evan N Feinberg, Joseph Gomes, Caleb Geniesse, Aneesh S Pappu, Karl Leswing, and Vijay Pande. Moleculenet: a benchmark for molecular machine learning. *Chemical science*, 9(2):513–530, 2018.

[100] Zonghan Wu, Shirui Pan, Fengwen Chen, Guodong Long, Chengqi Zhang, and S Yu Philip. A comprehensive survey on graph neural networks. *IEEE transactions on neural networks and learning systems*, 32(1):4–24, 2020.

[101] Yaochen Xie, Zhao Xu, Jingtun Zhang, Zhengyang Wang, and Shuiwang Ji. Self-supervised learning of graph neural networks: A unified review. *IEEE Transactions on Pattern Analysis and Machine Intelligence*, 2022.

[102] Keyulu Xu, Weihua Hu, Jure Leskovec, and Stefanie Jegelka. How powerful are graph neural networks? In *7th International Conference on Learning Representations, ICLR 2019, New Orleans, LA, USA, May 6-9, 2019*. OpenReview.net, 2019.

[103] Omry Yadan. Hydra - a framework for elegantly configuring complex applications. Github, 2019. URL https://github.com/facebookresearch/hydra.

[104] Xiang Yue, Zhen Wang, Jingong Huang, Srinivasan Parthasarathy, Soheil Moosavinasab, Yungui Huang, Simon M Lin, Wen Zhang, Ping Zhang, and Huan Sun. Graph embedding on biomedical networks: methods, applications and evaluations. *Bioinformatics*, 36(4):1241–1251, 2020.

[105] Dengyong Zhou, Olivier Bousquet, Thomas Lal, Jason Weston, and Bernhard Schölkopf. Learning with local and global consistency. *Advances in neural information processing systems*, 16, 2003.

[106] Jie Zhou, Ganqu Cui, Shengding Hu, Zhengyan Zhang, Cheng Yang, Zhiyuan Liu, Lifeng Wang, Changcheng Li, and Maosong Sun. Graph neural networks: A review of methods and applications. *AI Open*, 1:57–81, 2020.

[107] Kaixiong Zhou, Xiao Huang, Yuening Li, Daochen Zha, Rui Chen, and Xia Hu. Towards deeper graph neural networks with differentiable group normalization. *Advances in neural information processing systems*, 33:4917–4928, 2020.

[108] Marinka Zitnik and Jure Leskovec. Predicting multicellular function through multi-layer tissue networks. *Bioinformatics*, 33(14):i190–i198, 2017.

A Additional information

A.1 Example code for `obnb`

The `obnb` library provides high-level APIs for users to set up benchmarking datasets from diverse selections of gene interaction networks and gene annotations to study the performance of various graph learning methods. Below, we provide a simple code snippet demonstrating how to set up a full dataset in a single function call. Further, we demonstrate how the constructed dataset can be directly used to evaluate the performance of a simple GNN model. We also invite readers to check out the README file of the `obnb` library for more comprehensive example usages: https://github.com/krishnanlab/obnb/blob/main/README.md.

```python
from obnb.dataset import OpenBiomedNetBench

# Download the current processed archive (set version to "latest" to
# download data from source directly and process them from scratch)
dataset = OpenBiomedNetBench(root="datasets", version="current", graph_name="BioGRID",
                             label_name="DisGeNET", auto_generate_feature="OneHotLogDeg")

# User built-in GNN trainer to train and evaluat the performance of a simple GCN
gcn_model = GCN(in_channels=1, hidden_channels=64,
                num_layers=5, out_channels=dataset.num_tasks)
gcn_trainer = SimpleGNNTrainer(device="cuda", metric_best="apop")
gcn_results = gcn_trainer.train(gcn_model, dataset)

# Alternatively, convert the dataset into your favorite GNN framework, i.e., PyG or DGL
# Or use OpenBiomedNetBenchPyG or OpenBiomedNetBenchDGL to directly instantiate the dataset
pyg_data = dataset.to_pyg_data()
dgl_data = dataset.to_dgl_data()
```

Listing 1: Example code for using `obnb` to set up the BioGRID-DisGeNET benchmarking dataset.

A.2 Benchmarking experiments implementation information

The `obnbench` benchmarking codebase utilizes PyTorch [70] and PyTorch Geometric (PyG) [25] for building deep (graph) neural network models. In addition, we leverage Weights & Bias [10] for tracking training results and Hydra [103] for managing experiment configurations. All benchmarking experiments are run using computational nodes with five CPUs, 45GB memory, and a Tesla V100 GPU (32GB).

A.3 GNN backbone design

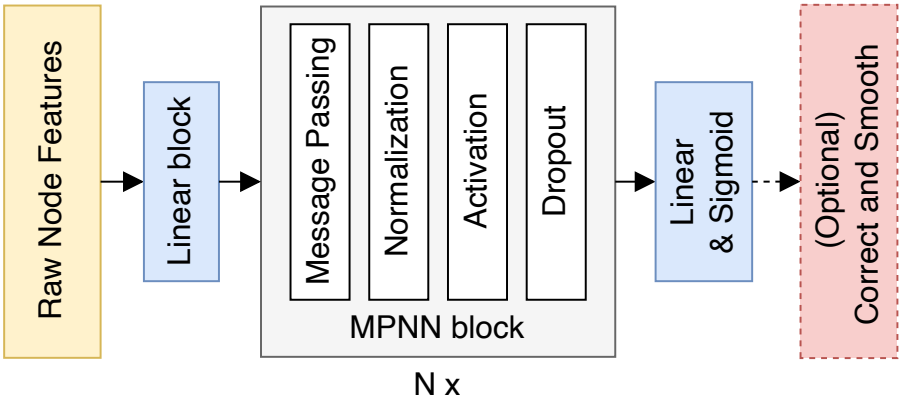

Figure S1: Model architecture overview

The basic GNN architecture we used contains the following components:

Feature encoder Since the genes do not come with canonical features, we need to derive initial node features for the GNN model. The default option we used is OneHotLogDeg with 32 bins (A.3.1). The raw features are first processed by a custom batch norm layer that is activated during testing in

addition to training. Then, the processed features are projected into the hidden dimension ($d = 128$ by default) of the model via a linear layer, followed by batch norm and ReLU activation.

Message passing layers We use five message passing layers in the GNN model by default. Each message passing layer contains a convolution block (A.3.2), followed by normalization, non-linear activation, and dropouts. We apply residual connection by summing up the input and the output of the graph convolution block.

Prediction head and post-processing Finally, we apply a linear layer to project the hidden dimension to the dimension matching the number of tasks and apply a sigmoid activation to turn the prediction into binary prediction probabilities. Optionally, we apply correct and smooth (C&S) [39] at test time to correct the predicted probabilities via a two-step label propagation (A.3.3).

A.3.1 Node feature design

In this section, we provide an overview of a diverse selection of node feature constructions we used in our benchmark. All node features are constructed using the whole network as input in a transductive setting, except for a few cases where the node features do not depend on the network structure, such as constant features. By default, any initial node feature will be 128-dimensional unless otherwise specified. We start by designing a collection of simple statistics that can be easily derived.

Constant uses a one-dimensional trivial feature for every node in the graph.

RandomNormal samples 32-dimensional features for each node independently via a standard normal distribution.

OneHotLogDeg (short for LogDeg) first computes the log degree of each node in the graph and then uniformly bins the nodes into one of 32 bins based on their log degree. The one-hot encoded node degrees approach has recently been shown to be a great structure encoder, whose utilization can sometimes result in performance superior to using the original node features associated with the graph [17, 55]. Meanwhile, the design choice of using log-uniform grids stems from the scale-free nature of biological networks [2].

RandomWalkDiag is the landing probability of a node back to itself after k hops, which is also commonly referred to as the random walk structural encodings (RWSE) [21]. It has been used widely in many graph transformer models due to its expressiveness in capturing graph structure [52]. Next, we consider several node feature options derived directly from the adjacency matrix.

Adj uses the rows of the adjacency matrix as the node feature. It has been shown previously [54] that logistic regression using the adjacency matrix produced better prediction performance than the commonly used label propagation algorithm for diverse gene classification problems.

RandProjGaussian and RandProjSparse are random projections of the adjacency matrix using two different but related approaches. We use the scikit-learn [71] implementations (`GaussianRandomProjection` and `SparseRandomProjection`) to compute these features.

SVD uses the left singular vectors of the adjacency matrix as the node features.

LapEigMap [9] uses the (ℓ_2 normalized) eigenvectors of the symmetric normalized graph Laplacian as the node features.

Node embeddings [68] are powerful approaches to extracting vectorial representations of each node in a graph and have shown promising results in many biomedical application [54, 104, 5]. Thus, we include a few popular and good-performing node embedding options in our benchmark.

LINE1 and LINE2 [87] extracts first- and second-order proximity information from the graph to train the underlying embeddings. We use the GraPE [15] implementation to compute the LINE embeddings.

Node2vec [31] extracts node representation using word2vec [64] on node sequences sampled from the graph via biased random walks. The biased random walks, in contrast to an earlier work, DeepWalk [74], which uses an unbiased search, allow the searching strategy to be more flexible, mimicking either breadth-first search or depth-first search in the random walk phase.

Walklets [75] is similar to botch Node2vec and DeepWalk in that it runs word2vec using random walks sampled from the graph. However, wallets sample node pairs from the random walk with a

specific number of hops, allowing a more explicit control of the multiscale relationships between nodes.

Finally, we experiment with options that let the model learn the node features freely.

Embedding lets the model learn the node features freely.

AdjEmbBag is similar to Embedding but with an additional aggregation step that sums up the raw embedding of each node from the central node's neighborhood.

A.3.2 Graph neural network summary

In this section, summarize the five tested GNN models under the message-passing framework [26]. Let h_i^l be the *raw* representation of vertex i at layer j, and $\tilde{h}_i^l$ be the corresponding *processed* representation, e.g., after non-linear activation and normalization. The message-passing framework is written as

$$h_i^{l+1} = f^l\Big(\bigoplus_{j\in\mathcal{N}_i} \phi_n^l(\tilde{h}_j^l), \phi_s^l(\tilde{h}_i^l)\Big) \tag{1}$$

where $\bigoplus$ is the aggregation operator, f is the update function, ϕ_n and ϕ_s are message functions for neighbors and self. Different GNNs differ in the choices of $\bigoplus$, f, ϕ_n and ϕ_s they use.

GCN [48] uses a scaled linear transformation as the message function. The scaling factor is computed as the normalized edge weights with added self-loop. The aggregation is done by summing up the transformed message functions.

$$h_i^{l+1} = \sum_{j\in\mathcal{N}_i}\Big(\frac{e_{i,j}}{\sqrt{\tilde{d}_i\tilde{d}_j}}\Theta^l\tilde{h}_j^l\Big) + \frac{e_{i,i}}{\tilde{d}_i}\Theta^l\tilde{h}_i^l \tag{2}$$

where $\tilde{d}_i = d_i + 1 = \sum_{j\in\mathcal{N}_i} e_{i,j}$ is the degree of vertex i with self-loop added.

SAGE [32] uses two separate linear transformations as the message functions for neighbors and self. The aggregation is done by taking the sum[1] of the neighbors' messages and then adding it to the self-message. We additionally use an affine update function to transform the aggregated messages.

$$h_i^{l+1} = \Theta_u^l\left(\Theta_n^l\Big(\sum_{j\in\mathcal{N}_i}\tilde{h}_j^l\Big) + \Theta_s^l\tilde{h}_i^l\right) + b_u^l \tag{3}$$

GIN [102] uses a multi-layer perceptron (MLP) to update the aggregated messages, which is done by summing up neighbors' representations and self-representation from the last layer.

$$h_i^{l+1} = \mathrm{MLP}^l\Big(\sum_{j\in\mathcal{N}_i}\tilde{h}_j^l + (1+\epsilon)\tilde{h}_i^l\Big) \tag{4}$$

GAT [90, 13] uses an attention mechanism to distribute the weights from which the linear transformed messages are aggregated.

$$h_i^{l+1} = \sum_{j\in\mathcal{N}_i}\Big(\alpha_{i,j}\Theta_v^l\tilde{h}_j^l\Big) + \alpha_{i,i}\Theta_v^l\tilde{h}_i^l \tag{5}$$

In particular, the original GAT paper [90] formulated the attention scores as follows

$$\alpha_{i,j} = \frac{\exp\Big(\mathrm{LeakyReLU}\big((a^l)^\top\Theta_a^l[\tilde{h}_i^l||\tilde{h}_j^l]\big)\Big)}{\sum_{k\in\mathcal{N}_i}\exp\Big(\mathrm{LeakyReLU}\big((a^l)^\top\Theta_a^l[\tilde{h}_i^l||\tilde{h}_k^l]\big)\Big)} \tag{6}$$

However, it was pointed out in a more recent work, GATv2 [13], that the above formulation was fundamentally limited in the types of attention the model can learn and proposed a correction that

[1]The original paper uses mean aggregation, but we found that sum aggregation works better in our benchmark.

showed stronger performances follow.

$$\alpha_{i,j} = \frac{\exp\left((a^l)^\top \text{LeakyReLU}\big(\Theta_a^l[\tilde{h}_i^l || \tilde{h}_j^l]\big)\right)}{\sum_{k\in\mathcal{N}_i}\exp\left((a^l)^\top \text{LeakyReLU}\big(\Theta_a^l[\tilde{h}_i^l || \tilde{h}_k^l]\big)\right)} \tag{7}$$

We also observe a slight but significant improvement when using GATv2 attention as opposed to the original GAT. Thus, all reported GAT results are based on v2 attention.

GatedGCN [12] uses gating mechanisms to process neighbors' messages, with linear transformations as the message functions. The aggregation is done by summing up the gated messages from neighbors and adding them to the self-message.

$$h_i^{l+1} = \sum_{j\in\mathcal{N}_i}\left(\eta_{i,j}\odot\Theta_v^l\tilde{h}_j^l\right) + \Theta_s^l\tilde{h}_i^l \tag{8}$$

where $\odot$ is the elementwise multiplication operator, and the gating coefficients $\eta_{i,j}$ are computed as

$$\eta_{i,j} = \text{sigmoid}\big(\Theta_q^l\tilde{h^l}_i + \Theta_k^l\tilde{h^l}_j\big) \tag{9}$$

A.3.3 Label propagation and C&S

Label propagation iteratively propagates the label information from the source nodes outwards through the network neighborhoods [49, 16, 66]. Let $\mathbf{Y}\in\{0,1\}^{n\times d}$ be the (training) label matrix, and $\mathbf{M}\in\mathbb{R}^{n\times n}$ be the diffusion operator. The propagated information at step t, denoted $\mathbf{F}_t\in\mathbb{R}^{n\times d}$, is defined as

$$\mathbf{F}_t = \alpha\mathbf{F}_{t-1} + (1-\alpha)\mathbf{F}_0 \tag{10}$$

where $\mathbf{F}_0 = \mathbf{F}$ is the features to be propagated, which is the label matrix $\mathbf{Y}$ in the case of label propagation. The propagated feature is computed by repeating the propagation above until convergence:

$$\text{PROPAGATE}(\mathbf{F}) = \lim_{t\to\infty}\mathbf{F}_t \tag{11}$$

In practice, equation 11 is approximated by applying the propagation until the changes are small enough.

The original label propagation paper [105] uses the symmetric normalized adjacency matrix $\mathbf{D}^{-1/2}\mathbf{A}\mathbf{D}^{-1/2}$ as the diffusion operator, where $\mathbf{A}$ and $\mathbf{D}$ are the adjacency matrix and the corresponding diagonal degree matrix. Here, we use the column stochastic matrix $\mathbf{D}^{-1}\mathbf{A}$ as the diffusion operator to resemble the random walk with restart (RWR) implementation that is more commonly used in the network biology literature [16]. We use a propagation parameter α of 0.1 (equivalent to a restart parameter of 0.9) for label propagation.

C&S implements the idea of using label propagation[2] to (1) correct for the error made by the model and (2) smooth out the corrected predictions. Specifically, let $\mathbf{E} = \mathbf{Y}_{\text{train}} - \mathbf{Z}$ be the prediction error matrix, where $\mathbf{Z}$ is the predicted probabilities resulting from the model. C&S can be summarized as follows.

1. Propagate the error matrix: $\tilde{\mathbf{E}} = \text{PROPAGATE}(\mathbf{E})$.
2. Correct the original prediction with a fixed scale s: $\tilde{\mathbf{Z}} = \mathbf{Z} + s\tilde{\mathbf{E}}$.
3. Smooth out the corrected predictions: $\mathbf{Z}_{\text{C\&S}} = \text{PROPAGATE}(\tilde{\mathbf{Z}})$

We use $\alpha = 1.0$ for the correction step, $\alpha = 0.8$ for the smoothing step, and a scaling factor of $s = 1.5$.

[2] Uses the symmetric normalized adjacency matrix for propagation.

A.4 Training and hyperparameter details

All hyperparameters are listed in the configuration files for each model in the benchmarking repository[3]. We summarize the primary default hyperparameters for GNN in Table S1.

For logistic regression baselines, we use the SGD optimizer with a constant learning rate of 200, weight decay of 1e-5, and momentum of 0.9.

A.4.1 Fully tuned GNN models

In addition to the baseline GNN experiments where we used the default settings elaborated above, we also tuned GCN and GAT specifically for the four primary benchmarks presented in the main paper with a bag of tricks (BoT). Specifically, we construct node features by concatenating Node2vec embeddings ($d = 128$), OneHotLogDeg encodings ($d = 32$), and LabelReuse. Finally, we apply correct and smooth (C&S) to the GNN predictions as a post-processing step.

We use the Bayesian search hyperparameter optimization strategy provided by Weights&Biases [10] and optimize for the validation APOP scores to tune the dataset-specific hyperparameters for GCN and GAT on primary results presented in Table 2. The search space is listed in Table S2 and the final hyperparameter settings are summarized in Table S3,S4.

Table S1: Default hyperparameter settings

	Parameter	Value
General architecture	Hidden dimensions	128
	Number of layers	5
	Activation	ReLU
	Dropout	0.2
	Normalization	DiffGroupNorm [107]
GAT specific	Heads	1
	Attention dropout	0.05
GIN specific	MLP layers	2
	MLP dimensions	256
	ϵ	0.0
Optimizer (AdamW [58])	Learning rate	0.01
	Weight decay	1e-6
	Max epochs	50,000
	Early stopping patience	500
Learning rate scheduler (ReduceLROnPlateau)	Scheduler patience	100
	Scheduler reduce factor	0.5
	Minimum learning rate	1e-5

Table S2: Hyperparameter search space for GCN and GAT on the primary datasets

Parameter	Search space
Number of layers	{1, 2, 3, 4, 5, 6, 7, 8}
Hidden dimensions	{64, 128, 192, 256}
Number of heads (GAT)	{1, 2, 3, 4}
Attention dropout (GAT)	{0.0, 0.05, 0.1}
Dropout	{0.1, 0.2, 0.3}
Normalization	{none, BatchNorm, LayerNorm, PairNorm, DiffGroupNorm}
Activation	{ReLU, PReLU, GELU, SELU, ELU}

A.5 The log2 fold change of average precision over the prior metric (APOP)

APOP is computed by taking log_2 of the ratio between the average precision and the prior. The prior is computed as the ratio between the number of positives and the total number of samples, which

[3] https://github.com/krishnanlab/obnbench/tree/main/conf

Table S3: Tuned GCN model on the four primary benchmarks.

	BioGRID		HumanNet	
	GOBP	DisGeNET	GOBP	DisGeNET
Hidden dimension	192	256	192	64
Number of layers	3	1	4	4
Activation	SELU	PReLU	GELU	ReLU
Dropout	0.3	0.3	0.3	0.3
Normalization	DiffGroupNorm	DiffGroupNorm	–	DiffGroupNorm

Table S4: Tuned GAT (v2) model on the four primary benchmarks.

	BioGRID		HumanNet	
	GOBP	DisGeNET	GOBP	DisGeNET
Hidden dimension	128	64	128	64
Number of layers	4	2	4	8
Number of heads	1	4	1	1
Attention dropout	0.05	0.1	0.1	0.1
Activation	SELU	PReLU	PReLU	GELU
Dropout	0.2	0.3	0.2	0.1
Normalization	BatchNorm	DiffGroupNorm	DiffGroupNorm	DiffGroupNorm

corresponds to the probability that a randomly drawn sample is positive. Thus, APOP indicates how much better (> 0), or worse (< 0), a prediction is than a random guess, in two-fold change. More precisely,

$$\text{APOP} = \log_2\left(\frac{\text{Average Precision}}{\text{prior}}\right) = \log_2\left(\frac{\sum_n (R_n - R_{n-1})P_n}{(\#\text{ positives})/(\#\text{ positives} + \#\text{ negatives})}\right) \quad (12)$$

where R_n and P_n are the recall and precision and precision at the n^{th} prediction score threshold.

The average precision is also related to the AUPRC[4], which has been shown to be more suitable than the AUROC[5] in the case of class imbalance [80, 83]. In our dataset, class imbalance is prevalent, where each class has only one or two hundred of positive examples but thousands of negative examples (Table 1b,S11). Moreover, AUROC is more tolerant of errors made on top predictions and generally only requires that the global distribution of the predictions made is consistent with the true labels. AUPRC and AP, on the other hand, penalize the top predictions' errors more.

Practical relevance The OBNB benchmarks cover diverse gene prioritization tasks, such as pinpointing relevant genes for a particular disease. This formulation can also be straightforwardly extend to drug recommendation or drug repurposing tasks, by considering known drug targets (genes) as positive examples. For such biomedicine applications, in practice, only a few top predictions made by a predictive method can be experimentally verified by experimentalists due to the high experimental costs. Thus, APOP's emphasis on top predictions is well-aligned with this practical constraint and encourages methods to make highly accurate top predictions.

A.6 Corrected Homophily Ratio

Let $G = (V, E, w)$ be a weighted graph (unweighted graphs can be treated as weighted graphs with identical edge weights), with node set V, edge set E, and the edge weight function $w : V \times V \to \mathbb{R}$. Let $y_i : V \to \{0, 1\}^p$ be the label function for the i^{th} class (or label), for $i \in \{1, \ldots, p\}$.

We define the set of *labeled nodes* V_{labeled} as the ones that are part of at least one label, i.e., $V_{\text{labeled}} = \{v \in V | \max_{i \in 1,\ldots,p} y_i(v) = 1\}$. Furthermore, we define the *positively* and *negatively labeled nodes* for the i^{th} class as $V^{(i+)}_{\text{labeled}} = \{v \in V | y_i(v) = 1\}$ and $V^{(i-)}_{\text{labeled}} = \{v \in V | y_i(v) = 0\}$, respectively

[4]The area under the precision and recall curve.

[5]The area under the receiver operator characteristic curve.

Definition 1 (Node homophily ratio)**.** *The node homophily ratio of the i^{th} class for node v is defined as the ratio of its neighborhood that is positively labeled in the i^{th} class.*

$$h_i(v) = \frac{|\{u \in \mathcal{N}(v) | y_i(u) = 1\}|}{|\mathcal{N}(v)|}$$

Definition 2 (Positive and negative homophily ratio)**.** *The positive and negative homophily ratios of the i^{th} class (or label) are defined as the ratio of a node's neighborhood that are positively labeled for the i^{th} class averaged over the positively and negatively labeled nodes, respectively*

$$h_{i+} = \frac{1}{|V_{labeled}^{(i+)}|} \sum_{v \in V_{labeled}^{(i+)}} h_i(v), \quad h_{i-} = \frac{1}{|V_{labeled}^{(i-)}|} \sum_{v \in V_{labeled}^{(i-)}} h_i(v)$$

We refer to the *positive homophily ratio* as the *homophily ratio* for short. Note that definition 1 is slightly different from the typical definition of node homophily that is used in previous works targeting multiclass classification settings [72]. Specifically, (1) we only count positive nodes from the neighborhood instead of nodes having the same class as the central node since we are dealing with (multilabel) binary classification, which will also come in handy later for defining the corrected homophily ratio; (2) we only average the node homophily ratios over the positive node sets since our datasets have a notable class imbalance, where most nodes are negatively labeled. This way, the homophily ratio is less skewed towards the majority of negatively labeled nodes.

Definition 3 (Corrected homophily ratio)**.** *The corrected homophily ratio of the i^{th} class is defined as the expected fold change of node homophily between positively and negatively labeled nodes for class i*

$$\tilde{h}_i = \log_2 \left(\frac{h_{i+}}{h_{i-}} \right)$$

This corrected homophily ratio provides an answer to the following question: *How much more likely are nodes labeled in class i to be connected with other nodes labeled in class i compared to nodes not labeled in class i*? A positive value of the corrected homophily ratio indicates that positive nodes in class i have a higher likelihood of interacting with other positive nodes of class i than with negative nodes.

A.7 Community standards and maintenance plans

We follow several community standards to ensure sustainable and maintainable community-wide contributions, which is the key to the continuing improvement of a code base. First, we release the code on GitHub `https://github.com/krishnanlab/obnb` under the permissive MIT license. Second, we use Sphinx to build the documentation of the code base and host it on ReadTheDocs.org. Several quick-start examples using the package are also provided on the GitHub README page. Third, code quality is ensured via various testing and code-linting automation using tox, pytest, pre-commit hooks, and GitHub actions. Fourth, we provide contribution guidelines and a code of conduct on the GitHub page. Finally, as a part of our commitment to the community, we also put in place a maintenance plan to address GitHub issues, merge pull requests, and release updates periodically to ensure the benchmarks remain adaptive to the evolving needs of the community.

B Data descriptions

B.1 Networks

BioGRID [85] (MIT License) is a protein interaction network curated from primary experimental evidence from the biomedical literature, as well as evidence inferred from low- and high-throughput experiments.

BioPlex [41] (Creative Commons Attribution-ShareAlike 4.0 International License) is a protein interaction network whose interactions are measured by affinity purification-mass spectrometry (AP-

MS) analysis shared across two cell lines (HEK293T and HCT116). This shared interaction network encodes core complexes involving many essential proteins that are vital for the cell's survival.

ComPPIHumanInt [92] (CC BY-NC 4.0 License) is a context-naive version of the cellular compartment-specific ComPPI [92] networks for humans, which are constructed by combining protein interactions from nine different PPI databases (including BioGRID).

ConsensusPathDB [46] (Free for academic use, see `http://cpdb.molgen.mpg.de/` for more Licensing info) integrates protein interaction evidence (binary protein interaction, protein complex interaction, genetic interaction, metabolic, signaling, etc.) from 31 public databases, in addition to interactions curated from the literature.

FunCoup [76] (CC BY-SA 4.0 License) version 5 is a functional gene interaction network constructed by integrating a wide range of interaction evidence using a redundancy-weighted naive Bayes approach.

HIPPIE [1] (CC BY-NC 4.0 License) integrates experimentally detected protein interactions from several public databases such as BioGRID.

HumanBaseTopGlobal [29] (CC BY 4.0 License) is the tissue-naive version of the HumanBase tissue-specific gene interaction network collections, which are constructed by integrating hundreds of thousands of publicly available gene expression studies, protein–protein interactions and protein–DNA interactions via a Bayesian approach, calibrated against high-quality manually curated functional gene interactions.

HuMAP [20] (CC0 1.0 License) is a protein interaction network derived from over seven thousand protein complexes by integrating experimental evidence from public resources including AP-MS, large-scale biochemical fraction data, proximity labeling, and RNA hairpin pulldown data.

HumanNet [42] (CC BY-SA 4.0 License) is a functional gene interaction network originally designed for disease studies. It contains interaction evidence from gene co-citation from the literature, gene co-expression, pathway, domain profile, genetic interaction, gene neighborhood, phylogenic profile, and other protein interaction data. All these interaction evidence are integrated using a Bayesian statistical framework, resulting in a single value for each pair of genes that indicate the odds ratio for their functional interaction.

HuRI [60] (CC BY-4.0 License) is a binary protein interaction network constructed via the yeast two-hybrid (Y2H), covering about 90% of the protein-coding genes in the human genome.

OmniPath [88] (See `https://omnipathdb.org/info` for Licenses collected for each database) integrates protein interactions, signaling and regulatory relationships from over 100 resources.

PCNet [36] (CC BY-NC 4.0 License) is a protein interaction network constructed by requiring that an edge be supported by at least two out of the 21 selected protein interaction networks, such as BioGRID and ConsensusPathDB.

ProteomeHD [50] (CC BY-4.0 License) is the subnetwork of [50] containing top 0.5% strongest co-regulation signal between pairs of proteins. The co-regulation is measured by proteins' response to a total of 294 biological perturbations via isotope-labeling mass spectrometry.

SIGNOR [73] (CC BY-4.0 License) contains manually curated causal signaling relationships between proteins and other biochemical molecules, such as transcriptional activations and phosphorylation.

STRING [86] (CC BY-4.0 License) is a functional interaction network constructed by integrating seven types of gene interaction evidence via a probabilistic approach that calibrates against the KEGG [47] pathway database. The seven evidence types include conserved neighborhood, gene co-occurrence across species, gene fusion events, gene co-expression, other databases, and text-mined interactions.

B.2 Annotations and Ontologies

Gene Ontology [4] (CC BY-4.0 License) is a structured and standardized system that provides a comprehensive vocabulary to describe the molecular functions (GOMF), biological processes (GOBP), and cellular components (GOCC) associated with genes across different organisms. It aims

to unify the representation of biological knowledge and enable effective analysis and interpretation of genomic data.

Mondo Disease Ontology [89] (CC BY-4.0 License) is a unifying resource that integrates disease, genotype, and phenotype knowledge across diverse resources, providing a standardized knowledge graph with controlled vocabularies for diseases and phenotypes.

DisGeNET disease gene annotations [77] (CC BY-NC 4.0 License) is a disease gene annotation database that contains a wide range of disease-gene association evidence, including curated annotations, high-throughput experiments and other inferred annotations, animal models, and literature text-mined annotation mostly from BEFREE. By default, we only use the curated and inferred annotations.

DISEASES disease gene annotations [30](CC BY License) is another disease gene annotation database that has a weekly update schedule for extracting disease gene annotations via text-mining from the fast-growing literature. The text-mined approach uses full text instead of only using the titles and abstracts. Other disease gene annotations from experimental data and other databases are also available.

B.3 Archived data

In addition to downloading and processing the data directly from the original sources, we also provide archived versions of the data preprocessed by use by running the default OBNB processing pipelines. The archived data is versioned with DOI's and can be found on Zenodo under the record `https://zenodo.org/record/8045270`

C Additional results

Table S5: Ablation study on different initial node feature constructions for GCN and GAT. Reported values are average test APOP scores aggregated over five random seeds. The best score within a group (network x label x model) is **bolded**.

Network	Model	Feature	DISEASES	DisGeNET	GOBP
BioGRID	GCN	Constant	0.373 ± 0.018	0.451 ± 0.210	0.557 ± 0.144
		RandomNormal	1.329 ± 0.043	0.867 ± 0.017	2.121 ± 0.114
		OneHotLogDeg	1.077 ± 0.057	0.827 ± 0.050	2.011 ± 0.148
		RandomWalkDiag	0.844 ± 0.103	0.702 ± 0.064	1.358 ± 0.044
		Adj	**1.442 ± 0.120**	0.899 ± 0.108	2.148 ± 0.045
		RandProjGaussian	1.288 ± 0.041	0.828 ± 0.034	2.278 ± 0.084
		RandProjSparse	1.264 ± 0.047	0.749 ± 0.057	2.306 ± 0.088
		SVD	1.259 ± 0.076	0.808 ± 0.030	2.318 ± 0.080
		LapEigMap	1.415 ± 0.030	0.963 ± 0.045	2.378 ± 0.098
		LINE1	1.258 ± 0.041	0.798 ± 0.023	2.376 ± 0.081
		LINE2	1.312 ± 0.027	0.857 ± 0.083	2.416 ± 0.048
		Node2vec	1.392 ± 0.051	**0.965 ± 0.055**	**2.487 ± 0.112**
		Walklets	1.366 ± 0.044	0.886 ± 0.079	2.438 ± 0.052
		Embedding	1.348 ± 0.073	0.788 ± 0.060	2.147 ± 0.113
		AdjEmbBag	1.338 ± 0.071	0.798 ± 0.080	2.031 ± 0.089
	GAT	Constant	0.399 ± 0.039	0.362 ± 0.071	0.398 ± 0.071
		RandomNormal	1.290 ± 0.126	0.755 ± 0.140	2.268 ± 0.047
		OneHotLogDeg	0.946 ± 0.289	0.803 ± 0.066	2.181 ± 0.080
		RandomWalkDiag	0.873 ± 0.115	0.554 ± 0.160	1.702 ± 0.068
		Adj	1.290 ± 0.320	0.594 ± 0.154	1.972 ± 0.230
		RandProjGaussian	1.357 ± 0.073	0.897 ± 0.070	2.402 ± 0.081
		RandProjSparse	1.351 ± 0.091	0.842 ± 0.063	2.461 ± 0.062
		SVD	1.019 ± 0.199	0.700 ± 0.081	2.384 ± 0.058
		LapEigMap	1.423 ± 0.072	**0.914 ± 0.103**	2.541 ± 0.042
		LINE1	**1.480 ± 0.073**	0.874 ± 0.071	2.486 ± 0.040
		LINE2	1.454 ± 0.043	0.888 ± 0.057	2.463 ± 0.138
		Node2vec	1.416 ± 0.126	0.877 ± 0.032	**2.585 ± 0.052**
		Walklets	1.464 ± 0.072	0.852 ± 0.073	2.392 ± 0.170
		Embedding	1.375 ± 0.092	0.834 ± 0.056	2.279 ± 0.197
		AdjEmbBag	0.645 ± 0.049	0.525 ± 0.041	1.242 ± 0.062
HumanNet	GCN	Constant	0.385 ± 0.018	0.898 ± 0.873	0.610 ± 0.037
		RandomNormal	3.006 ± 0.112	2.511 ± 0.031	3.302 ± 0.104
		OneHotLogDeg	2.873 ± 0.134	2.552 ± 0.059	3.574 ± 0.116
		RandomWalkDiag	2.056 ± 0.102	1.672 ± 0.171	3.001 ± 0.149
		Adj	**3.562 ± 0.049**	2.788 ± 0.096	3.715 ± 0.077
		RandProjGaussian	3.346 ± 0.096	2.768 ± 0.036	3.654 ± 0.054
		RandProjSparse	3.341 ± 0.085	2.784 ± 0.021	3.759 ± 0.039
		SVD	3.211 ± 0.062	2.723 ± 0.064	3.780 ± 0.075
		LapEigMap	3.219 ± 0.077	2.676 ± 0.072	3.735 ± 0.068
		LINE1	2.883 ± 0.097	2.560 ± 0.049	3.700 ± 0.078
		LINE2	2.918 ± 0.070	2.563 ± 0.082	3.656 ± 0.038
		Node2vec	3.359 ± 0.070	**2.798 ± 0.024**	3.816 ± 0.039
		Walklets	3.464 ± 0.066	2.762 ± 0.053	**3.842 ± 0.052**
		Embedding	3.389 ± 0.051	2.637 ± 0.032	3.538 ± 0.040
		AdjEmbBag	3.499 ± 0.032	2.700 ± 0.066	3.482 ± 0.048
	GAT	Constant	0.280 ± 0.043	0.449 ± 0.047	0.333 ± 0.035
		RandomNormal	3.442 ± 0.331	2.758 ± 0.204	3.535 ± 0.126
		OneHotLogDeg	3.052 ± 0.312	2.605 ± 0.074	3.661 ± 0.088
		RandomWalkDiag	2.623 ± 0.862	2.340 ± 0.285	3.409 ± 0.059
		Adj	**3.791 ± 0.071**	2.943 ± 0.053	3.770 ± 0.029
		RandProjGaussian	3.390 ± 0.105	2.749 ± 0.134	3.803 ± 0.103
		RandProjSparse	3.477 ± 0.135	2.811 ± 0.126	3.773 ± 0.085
		SVD	3.691 ± 0.080	2.653 ± 0.101	3.792 ± 0.076
		LapEigMap	3.438 ± 0.269	2.837 ± 0.180	3.907 ± 0.034
		LINE1	3.630 ± 0.058	2.794 ± 0.163	3.857 ± 0.085

		LINE2	3.430 ± 0.133	2.867 ± 0.051	3.779 ± 0.123
		Node2vec	3.662 ± 0.036	**2.975 ± 0.027**	**3.947 ± 0.090**
		Walklets	3.483 ± 0.103	2.887 ± 0.092	3.885 ± 0.112
		Embedding	3.539 ± 0.227	2.797 ± 0.087	3.738 ± 0.090
		AdjEmbBag	3.592 ± 0.086	2.802 ± 0.065	3.692 ± 0.075
ComPPIHumanInt	GCN	Constant	0.263 ± 0.026	0.307 ± 0.014	0.440 ± 0.039
		RandomNormal	1.544 ± 0.024	1.075 ± 0.058	2.411 ± 0.064
		OneHotLogDeg	1.394 ± 0.077	0.964 ± 0.043	2.244 ± 0.072
		RandomWalkDiag	0.946 ± 0.109	0.759 ± 0.053	1.652 ± 0.081
		Adj	1.471 ± 0.024	1.037 ± 0.074	2.320 ± 0.049
		RandProjGaussian	1.527 ± 0.067	1.069 ± 0.071	2.649 ± 0.030
		RandProjSparse	1.558 ± 0.069	1.030 ± 0.046	2.593 ± 0.058
		SVD	1.459 ± 0.026	**1.112 ± 0.056**	2.622 ± 0.091
		LapEigMap	**1.626 ± 0.037**	1.110 ± 0.061	2.484 ± 0.058
		LINE1	1.536 ± 0.103	1.057 ± 0.049	2.540 ± 0.049
		LINE2	1.606 ± 0.062	1.060 ± 0.041	2.588 ± 0.016
		Node2vec	1.546 ± 0.080	1.072 ± 0.047	**2.744 ± 0.067**
		Walklets	1.564 ± 0.053	1.086 ± 0.054	2.593 ± 0.034
		Embedding	1.356 ± 0.040	0.863 ± 0.068	2.190 ± 0.065
		AdjEmbBag	1.390 ± 0.042	0.929 ± 0.071	2.366 ± 0.080
	GAT	Constant	0.323 ± 0.052	0.327 ± 0.056	0.366 ± 0.047
		RandomNormal	1.386 ± 0.072	1.171 ± 0.107	2.584 ± 0.079
		OneHotLogDeg	1.287 ± 0.148	0.756 ± 0.272	2.197 ± 0.222
		RandomWalkDiag	1.197 ± 0.097	0.811 ± 0.044	1.933 ± 0.211
		Adj	1.348 ± 0.198	0.791 ± 0.095	2.087 ± 0.035
		RandProjGaussian	1.565 ± 0.027	1.074 ± 0.065	2.706 ± 0.107
		RandProjSparse	1.562 ± 0.067	1.107 ± 0.029	2.728 ± 0.068
		SVD	1.382 ± 0.076	1.050 ± 0.054	2.730 ± 0.058
		LapEigMap	1.622 ± 0.044	1.192 ± 0.043	2.742 ± 0.072
		LINE1	**1.633 ± 0.055**	1.134 ± 0.071	2.625 ± 0.085
		LINE2	1.569 ± 0.034	1.112 ± 0.067	2.656 ± 0.071
		Node2vec	1.572 ± 0.064	1.169 ± 0.079	2.766 ± 0.064
		Walklets	1.623 ± 0.028	**1.188 ± 0.070**	**2.789 ± 0.043**
		Embedding	1.544 ± 0.036	1.011 ± 0.082	2.487 ± 0.072
		AdjEmbBag	0.887 ± 0.078	0.611 ± 0.061	1.724 ± 0.066
BioPlex	GCN	Constant	0.342 ± 0.032	0.356 ± 0.052	0.488 ± 0.083
		RandomNormal	**1.304 ± 0.016**	0.868 ± 0.030	2.445 ± 0.064
		OneHotLogDeg	1.225 ± 0.065	**0.909 ± 0.050**	2.500 ± 0.044
		RandomWalkDiag	1.242 ± 0.043	0.835 ± 0.038	2.461 ± 0.138
		Adj	1.182 ± 0.067	0.817 ± 0.023	**2.613 ± 0.078**
		RandProjGaussian	1.218 ± 0.030	0.855 ± 0.066	2.583 ± 0.061
		RandProjSparse	1.256 ± 0.085	0.869 ± 0.017	2.563 ± 0.053
		SVD	1.273 ± 0.055	0.707 ± 0.046	2.513 ± 0.036
		LapEigMap	1.206 ± 0.038	0.785 ± 0.057	2.382 ± 0.026
		LINE1	1.234 ± 0.028	0.790 ± 0.033	2.604 ± 0.073
		LINE2	1.242 ± 0.059	0.789 ± 0.053	2.544 ± 0.060
		Node2vec	1.206 ± 0.042	0.784 ± 0.060	2.549 ± 0.074
		Walklets	1.215 ± 0.060	0.817 ± 0.045	2.558 ± 0.065
		Embedding	1.157 ± 0.024	0.772 ± 0.066	2.582 ± 0.034
		AdjEmbBag	1.240 ± 0.038	0.770 ± 0.021	2.582 ± 0.100
	GAT	Constant	0.275 ± 0.063	0.275 ± 0.146	0.569 ± 0.143
		RandomNormal	1.256 ± 0.070	0.884 ± 0.047	2.489 ± 0.063
		OneHotLogDeg	1.089 ± 0.100	0.793 ± 0.044	2.479 ± 0.098
		RandomWalkDiag	1.041 ± 0.082	0.788 ± 0.090	2.430 ± 0.085
		Adj	1.157 ± 0.029	0.811 ± 0.042	2.582 ± 0.069
		RandProjGaussian	1.222 ± 0.064	**0.924 ± 0.041**	2.588 ± 0.094
		RandProjSparse	1.213 ± 0.041	0.882 ± 0.063	**2.632 ± 0.009**
		SVD	1.139 ± 0.089	0.721 ± 0.073	2.539 ± 0.045
		LapEigMap	1.204 ± 0.062	0.832 ± 0.058	2.371 ± 0.064
		LINE1	1.201 ± 0.060	0.802 ± 0.035	2.453 ± 0.074
		LINE2	**1.242 ± 0.034**	0.850 ± 0.035	2.478 ± 0.057
		Node2vec	1.229 ± 0.039	0.768 ± 0.042	2.369 ± 0.061

		Walklets	1.196 ± 0.027	0.855 ± 0.073	2.531 ± 0.059
		Embedding	1.159 ± 0.044	0.746 ± 0.088	2.493 ± 0.071
		AdjEmbBag	1.183 ± 0.043	0.784 ± 0.050	2.522 ± 0.056
HuRI	GCN	Constant	0.346 ± 0.015	0.529 ± 0.033	0.384 ± 0.055
		RandomNormal	0.504 ± 0.108	0.676 ± 0.080	0.956 ± 0.125
		OneHotLogDeg	0.552 ± 0.080	0.579 ± 0.076	1.047 ± 0.102
		RandomWalkDiag	0.549 ± 0.107	0.484 ± 0.045	1.027 ± 0.129
		Adj	0.587 ± 0.023	0.631 ± 0.032	0.942 ± 0.075
		RandProjGaussian	0.676 ± 0.070	0.673 ± 0.046	1.016 ± 0.186
		RandProjSparse	**0.686 ± 0.087**	0.689 ± 0.055	1.076 ± 0.101
		SVD	0.628 ± 0.056	0.667 ± 0.010	1.005 ± 0.049
		LapEigMap	0.581 ± 0.014	0.526 ± 0.045	0.997 ± 0.085
		LINE1	0.658 ± 0.069	0.690 ± 0.054	1.053 ± 0.089
		LINE2	0.632 ± 0.125	**0.741 ± 0.074**	1.106 ± 0.084
		Node2vec	0.566 ± 0.061	0.738 ± 0.053	1.126 ± 0.114
		Walklets	0.596 ± 0.078	0.681 ± 0.032	**1.179 ± 0.056**
		Embedding	0.572 ± 0.070	0.606 ± 0.034	0.888 ± 0.109
		AdjEmbBag	0.652 ± 0.039	0.660 ± 0.030	1.059 ± 0.076
	GAT	Constant	0.305 ± 0.078	0.393 ± 0.077	0.345 ± 0.060
		RandomNormal	0.524 ± 0.159	0.541 ± 0.131	0.968 ± 0.114
		OneHotLogDeg	0.465 ± 0.060	0.510 ± 0.053	0.872 ± 0.189
		RandomWalkDiag	0.473 ± 0.057	0.445 ± 0.129	0.972 ± 0.057
		Adj	**0.683 ± 0.109**	0.528 ± 0.053	0.956 ± 0.157
		RandProjGaussian	0.592 ± 0.086	0.530 ± 0.071	1.028 ± 0.139
		RandProjSparse	0.603 ± 0.115	0.456 ± 0.085	1.017 ± 0.064
		SVD	0.522 ± 0.099	0.412 ± 0.029	1.021 ± 0.099
		LapEigMap	0.599 ± 0.082	0.557 ± 0.048	1.071 ± 0.080
		LINE1	0.585 ± 0.068	0.652 ± 0.043	1.101 ± 0.033
		LINE2	0.634 ± 0.067	**0.743 ± 0.053**	1.095 ± 0.054
		Node2vec	0.577 ± 0.017	0.657 ± 0.067	**1.116 ± 0.129**
		Walklets	0.630 ± 0.065	0.602 ± 0.032	1.085 ± 0.085
		Embedding	0.647 ± 0.087	0.601 ± 0.020	0.941 ± 0.081
		AdjEmbBag	0.603 ± 0.056	0.581 ± 0.040	0.902 ± 0.059
OmniPath	GCN	Constant	0.415 ± 0.083	0.416 ± 0.044	0.451 ± 0.046
		RandomNormal	1.417 ± 0.042	0.910 ± 0.126	1.798 ± 0.073
		OneHotLogDeg	1.195 ± 0.041	0.930 ± 0.046	1.753 ± 0.090
		RandomWalkDiag	0.847 ± 0.038	0.762 ± 0.045	1.427 ± 0.056
		Adj	**1.444 ± 0.019**	**1.118 ± 0.062**	2.050 ± 0.049
		RandProjGaussian	1.381 ± 0.089	1.014 ± 0.053	1.935 ± 0.075
		RandProjSparse	1.338 ± 0.073	1.066 ± 0.060	1.935 ± 0.020
		SVD	1.281 ± 0.052	0.849 ± 0.024	1.884 ± 0.048
		LapEigMap	1.408 ± 0.030	1.108 ± 0.092	**2.120 ± 0.040**
		LINE1	1.366 ± 0.075	0.946 ± 0.049	2.027 ± 0.042
		LINE2	1.338 ± 0.065	0.963 ± 0.054	1.938 ± 0.096
		Node2vec	1.384 ± 0.046	1.024 ± 0.020	1.982 ± 0.054
		Walklets	1.433 ± 0.050	1.036 ± 0.041	2.101 ± 0.033
		Embedding	1.329 ± 0.062	0.831 ± 0.069	1.504 ± 0.048
		AdjEmbBag	1.373 ± 0.042	1.085 ± 0.024	1.917 ± 0.054
	GAT	Constant	0.353 ± 0.044	0.343 ± 0.077	0.381 ± 0.053
		RandomNormal	1.374 ± 0.041	1.034 ± 0.091	1.945 ± 0.104
		OneHotLogDeg	0.775 ± 0.142	0.773 ± 0.135	1.685 ± 0.110
		RandomWalkDiag	0.754 ± 0.171	0.657 ± 0.159	1.580 ± 0.181
		Adj	**1.257 ± 0.179**	**1.184 ± 0.068**	1.865 ± 0.095
		RandProjGaussian	1.146 ± 0.117	1.032 ± 0.041	2.079 ± 0.126
		RandProjSparse	1.216 ± 0.075	0.916 ± 0.121	2.023 ± 0.272
		SVD	1.032 ± 0.125	0.889 ± 0.061	1.916 ± 0.159
		LapEigMap	1.344 ± 0.052	1.103 ± 0.087	2.105 ± 0.061
		LINE1	1.263 ± 0.082	0.936 ± 0.035	2.077 ± 0.108
		LINE2	1.376 ± 0.041	1.031 ± 0.104	2.026 ± 0.081
		Node2vec	1.317 ± 0.040	1.014 ± 0.090	2.096 ± 0.063
		Walklets	1.248 ± 0.099	1.022 ± 0.059	**2.190 ± 0.052**
		Embedding	1.371 ± 0.032	0.917 ± 0.103	1.738 ± 0.023

		AdjEmbBag	0.752 ± 0.076	0.724 ± 0.140	1.399 ± 0.171
ProteomeHD	GCN	Constant	0.289 ± 0.112	0.489 ± 0.021	0.729 ± 0.481
		RandomNormal	0.695 ± 0.128	0.583 ± 0.060	1.267 ± 0.074
		OneHotLogDeg	0.698 ± 0.060	0.692 ± 0.018	1.413 ± 0.078
		RandomWalkDiag	0.645 ± 0.072	0.665 ± 0.053	1.247 ± 0.049
		Adj	0.656 ± 0.060	0.588 ± 0.067	1.386 ± 0.054
		RandProjGaussian	0.617 ± 0.096	**0.714 ± 0.070**	1.412 ± 0.089
		RandProjSparse	0.685 ± 0.074	0.669 ± 0.084	1.461 ± 0.112
		SVD	**0.809 ± 0.073**	0.575 ± 0.081	1.474 ± 0.073
		LapEigMap	0.715 ± 0.017	0.535 ± 0.090	1.272 ± 0.035
		LINE1	0.588 ± 0.061	0.594 ± 0.042	1.316 ± 0.082
		LINE2	0.646 ± 0.071	0.630 ± 0.034	1.323 ± 0.073
		Node2vec	0.682 ± 0.049	0.621 ± 0.071	1.379 ± 0.102
		Walklets	0.635 ± 0.093	0.649 ± 0.082	1.400 ± 0.141
		Embedding	0.687 ± 0.074	0.539 ± 0.024	1.293 ± 0.158
		AdjEmbBag	0.600 ± 0.096	0.621 ± 0.123	**1.480 ± 0.083**
	GAT	Constant	0.375 ± 0.158	0.473 ± 0.082	0.675 ± 0.233
		RandomNormal	0.655 ± 0.115	0.657 ± 0.129	1.458 ± 0.049
		OneHotLogDeg	0.705 ± 0.115	0.687 ± 0.063	1.339 ± 0.199
		RandomWalkDiag	0.700 ± 0.065	0.691 ± 0.077	1.196 ± 0.277
		Adj	0.731 ± 0.149	0.625 ± 0.068	1.487 ± 0.080
		RandProjGaussian	0.808 ± 0.118	0.701 ± 0.036	1.491 ± 0.102
		RandProjSparse	0.725 ± 0.130	0.710 ± 0.061	1.502 ± 0.080
		SVD	0.792 ± 0.137	**0.828 ± 0.039**	**1.556 ± 0.057**
		LapEigMap	0.678 ± 0.041	0.534 ± 0.135	1.394 ± 0.079
		LINE1	0.638 ± 0.159	0.627 ± 0.094	1.338 ± 0.120
		LINE2	0.579 ± 0.079	0.599 ± 0.115	1.433 ± 0.076
		Node2vec	**0.839 ± 0.100**	0.702 ± 0.075	1.446 ± 0.089
		Walklets	0.644 ± 0.106	0.653 ± 0.098	1.544 ± 0.064
		Embedding	0.650 ± 0.141	0.659 ± 0.100	1.460 ± 0.041
		AdjEmbBag	0.685 ± 0.064	0.666 ± 0.079	1.408 ± 0.052
SIGNOR	GCN	Constant	0.388 ± 0.066	0.425 ± 0.157	0.500 ± 0.148
		RandomNormal	1.478 ± 0.050	1.349 ± 0.080	1.571 ± 0.056
		OneHotLogDeg	1.427 ± 0.032	1.183 ± 0.087	1.754 ± 0.066
		RandomWalkDiag	1.268 ± 0.011	1.022 ± 0.043	1.601 ± 0.127
		Adj	1.461 ± 0.042	1.306 ± 0.058	1.575 ± 0.087
		RandProjGaussian	1.488 ± 0.046	1.253 ± 0.083	1.764 ± 0.062
		RandProjSparse	1.535 ± 0.067	1.369 ± 0.107	1.780 ± 0.071
		SVD	1.396 ± 0.093	1.279 ± 0.071	1.788 ± 0.066
		LapEigMap	**1.597 ± 0.035**	1.345 ± 0.042	1.746 ± 0.057
		LINE1	1.546 ± 0.068	1.354 ± 0.049	1.813 ± 0.101
		LINE2	1.506 ± 0.084	**1.390 ± 0.103**	1.708 ± 0.076
		Node2vec	1.566 ± 0.071	1.345 ± 0.068	**1.887 ± 0.115**
		Walklets	1.562 ± 0.076	1.333 ± 0.088	1.732 ± 0.049
		Embedding	1.396 ± 0.035	1.200 ± 0.076	1.498 ± 0.064
		AdjEmbBag	1.496 ± 0.071	1.229 ± 0.130	1.665 ± 0.100
	GAT	Constant	0.279 ± 0.038	0.242 ± 0.051	0.488 ± 0.176
		RandomNormal	1.603 ± 0.049	1.281 ± 0.060	1.707 ± 0.050
		OneHotLogDeg	1.180 ± 0.069	1.009 ± 0.087	1.576 ± 0.047
		RandomWalkDiag	1.185 ± 0.115	0.935 ± 0.151	1.759 ± 0.115
		Adj	1.538 ± 0.104	1.251 ± 0.023	1.529 ± 0.053
		RandProjGaussian	1.531 ± 0.085	1.382 ± 0.107	1.751 ± 0.037
		RandProjSparse	1.508 ± 0.033	1.290 ± 0.073	1.715 ± 0.090
		SVD	1.529 ± 0.048	1.178 ± 0.102	1.718 ± 0.017
		LapEigMap	1.578 ± 0.053	1.326 ± 0.059	1.749 ± 0.081
		LINE1	1.583 ± 0.036	1.282 ± 0.052	1.844 ± 0.071
		LINE2	**1.630 ± 0.038**	1.325 ± 0.083	**1.863 ± 0.048**
		Node2vec	1.519 ± 0.066	1.287 ± 0.047	1.807 ± 0.033
		Walklets	1.579 ± 0.045	**1.411 ± 0.025**	1.762 ± 0.052
		Embedding	1.474 ± 0.095	1.254 ± 0.051	1.695 ± 0.053
		AdjEmbBag	1.457 ± 0.198	1.154 ± 0.096	1.405 ± 0.156

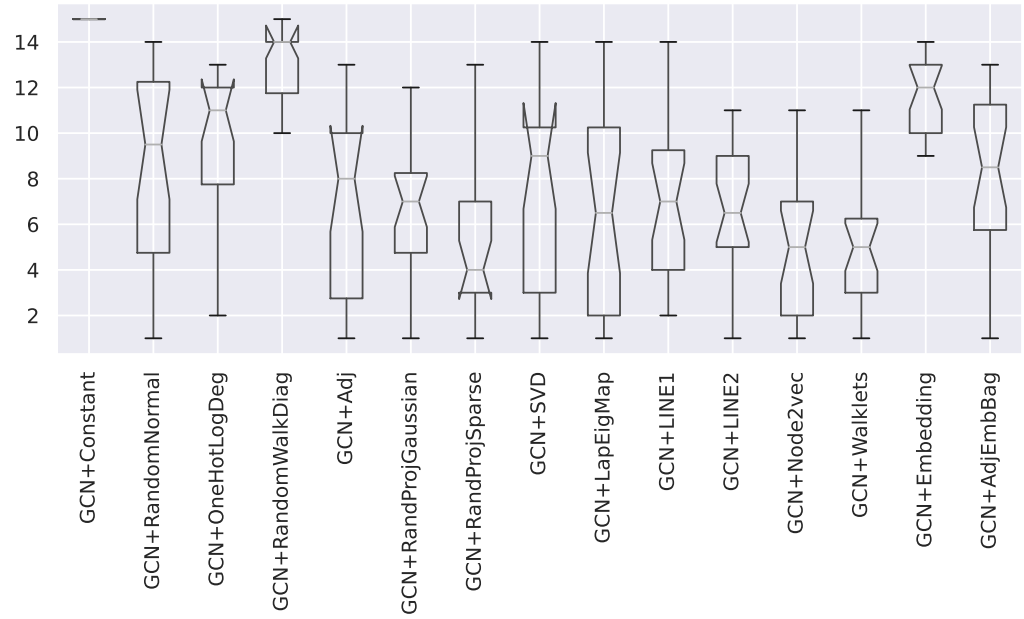

(a) GCN

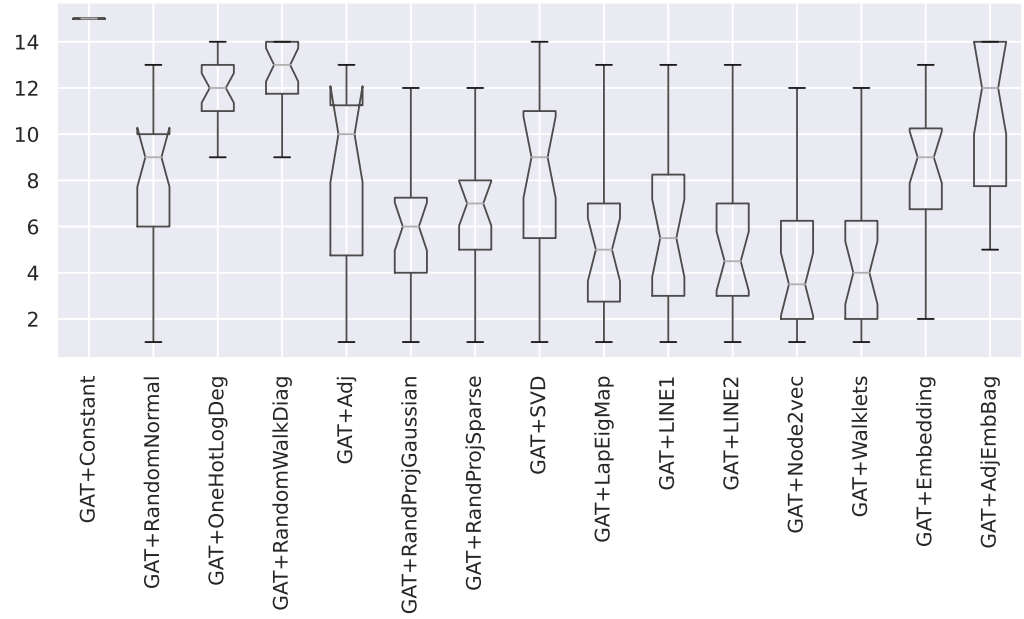

(b) GAT

Figure S2: **Boxplots representing the rankings of different feature construction when used by GNNs (lower the better).** Each point in a box is a ranking of a particular node feature construction on a specific dataset. A lower rank indicates that the particular node feature achieved higher test performance than others. For both GCN and GAT, *node2vec* appears to be the top-ranked node feature overall.

Table S6: **Baseline performance reference**. Reported values are average test APOP scores aggregated over five random seeds. The best performance achieved by (1) GNNs or (2) logistic regression and label propagation are **bolded** for each dataset (network × label). The best performance across the two methods groups is additionally colored by **green**.

Network	Model	Feature	DISEASES	DisGeNET	GOBP
BioGRID	GCN	OneHotLogDeg	**1.111 ± 0.043**	**0.773 ± 0.035**	**2.022 ± 0.100**
	SAGE	OneHotLogDeg	0.840 ± 0.105	0.665 ± 0.071	1.510 ± 0.114
	GIN	OneHotLogDeg	0.720 ± 0.061	0.700 ± 0.050	1.443 ± 0.120
	GAT	OneHotLogDeg	0.946 ± 0.289	0.552 ± 0.111	1.592 ± 0.408
	GatedGCN	OneHotLogDeg	1.014 ± 0.065	0.753 ± 0.047	1.924 ± 0.055
	LabelProp	–	1.210 ± 0.000	**0.931 ± 0.000**	1.885 ± 0.000
	LogReg	Adj	**1.328 ± 0.001**	0.743 ± 0.000	**2.528 ± 0.000**
	LogReg	LapEigMap	1.288 ± 0.001	0.864 ± 0.002	2.149 ± 0.000
	LogReg	SVD	0.881 ± 0.010	0.724 ± 0.003	2.088 ± 0.003
	LogReg	LINE1	1.117 ± 0.024	0.722 ± 0.004	2.264 ± 0.019
	LogReg	LINE2	1.132 ± 0.021	0.825 ± 0.007	2.351 ± 0.017
	LogReg	Node2vec	1.116 ± 0.054	0.836 ± 0.029	2.571 ± 0.015
	LogReg	Walklets	1.023 ± 0.052	0.786 ± 0.046	2.189 ± 0.020
HumanNet	GCN	OneHotLogDeg	2.902 ± 0.050	2.452 ± 0.107	3.524 ± 0.061
	SAGE	OneHotLogDeg	2.850 ± 0.107	2.356 ± 0.093	3.326 ± 0.067
	GIN	OneHotLogDeg	2.378 ± 0.126	2.019 ± 0.113	3.151 ± 0.017
	GAT	OneHotLogDeg	**3.052 ± 0.312**	**2.547 ± 0.207**	**3.571 ± 0.159**
	GatedGCN	OneHotLogDeg	3.004 ± 0.132	2.327 ± 0.026	3.486 ± 0.047
	LabelProp	–	3.728 ± 0.000	**3.059 ± 0.000**	3.806 ± 0.000
	LogReg	Adj	**3.812 ± 0.000**	3.053 ± 0.000	3.964 ± 0.006
	LogReg	LapEigMap	2.737 ± 0.003	2.301 ± 0.000	3.778 ± 0.001
	LogReg	SVD	2.785 ± 0.002	2.412 ± 0.004	3.618 ± 0.001
	LogReg	LINE1	2.178 ± 0.010	1.632 ± 0.005	3.348 ± 0.011
	LogReg	LINE2	2.270 ± 0.016	1.679 ± 0.005	3.485 ± 0.004
	LogReg	Node2vec	3.316 ± 0.020	2.433 ± 0.029	**4.036 ± 0.019**
	LogReg	Walklets	2.670 ± 0.069	2.050 ± 0.115	3.081 ± 0.054
ComPPIHumanInt	GCN	OneHotLogDeg	**1.359 ± 0.094**	**0.993 ± 0.042**	**2.251 ± 0.064**
	SAGE	OneHotLogDeg	1.101 ± 0.063	0.724 ± 0.076	1.865 ± 0.091
	GIN	OneHotLogDeg	0.963 ± 0.057	0.777 ± 0.057	1.621 ± 0.077
	GAT	OneHotLogDeg	1.287 ± 0.148	0.756 ± 0.272	2.197 ± 0.222
	GatedGCN	OneHotLogDeg	1.166 ± 0.045	0.861 ± 0.050	2.044 ± 0.094
	LabelProp	–	1.352 ± 0.000	**1.106 ± 0.000**	2.076 ± 0.000
	LogReg	Adj	**1.431 ± 0.000**	1.016 ± 0.000	2.707 ± 0.002
	LogReg	LapEigMap	1.257 ± 0.001	1.045 ± 0.005	2.177 ± 0.002
	LogReg	SVD	0.888 ± 0.003	0.702 ± 0.001	1.999 ± 0.002
	LogReg	LINE1	1.135 ± 0.023	0.905 ± 0.014	2.438 ± 0.019
	LogReg	LINE2	1.185 ± 0.021	0.895 ± 0.012	2.495 ± 0.024
	LogReg	Node2vec	1.341 ± 0.034	1.074 ± 0.005	**2.806 ± 0.049**
	LogReg	Walklets	1.073 ± 0.053	0.890 ± 0.032	2.109 ± 0.104
BioPlex	GCN	OneHotLogDeg	**1.277 ± 0.034**	**0.895 ± 0.046**	**2.535 ± 0.065**
	SAGE	OneHotLogDeg	1.118 ± 0.043	0.787 ± 0.049	2.215 ± 0.084
	GIN	OneHotLogDeg	1.182 ± 0.083	0.822 ± 0.086	2.360 ± 0.054
	GAT	OneHotLogDeg	1.089 ± 0.100	0.793 ± 0.044	2.479 ± 0.098
	GatedGCN	OneHotLogDeg	0.970 ± 0.049	0.723 ± 0.052	2.303 ± 0.114
	LabelProp	–	0.964 ± 0.000	0.556 ± 0.000	2.174 ± 0.000
	LogReg	Adj	1.087 ± 0.003	0.838 ± 0.011	2.467 ± 0.001
	LogReg	LapEigMap	**1.147 ± 0.005**	**0.903 ± 0.019**	2.298 ± 0.017
	LogReg	SVD	0.824 ± 0.006	0.588 ± 0.001	2.170 ± 0.022
	LogReg	LINE1	0.914 ± 0.062	0.653 ± 0.011	**2.475 ± 0.042**
	LogReg	LINE2	0.843 ± 0.050	0.627 ± 0.015	2.321 ± 0.015
	LogReg	Node2vec	0.816 ± 0.073	0.639 ± 0.053	2.194 ± 0.039
	LogReg	Walklets	0.742 ± 0.067	0.688 ± 0.053	1.822 ± 0.046
HuRI	GCN	OneHotLogDeg	0.529 ± 0.075	**0.625 ± 0.089**	**1.040 ± 0.049**
	SAGE	OneHotLogDeg	0.491 ± 0.083	0.541 ± 0.029	0.937 ± 0.048

	GIN	OneHotLogDeg	0.591 ± 0.089	0.477 ± 0.052	1.008 ± 0.113
	GAT	OneHotLogDeg	0.465 ± 0.060	0.510 ± 0.053	0.872 ± 0.189
	GatedGCN	OneHotLogDeg	**0.602 ± 0.090**	0.591 ± 0.098	0.957 ± 0.074
	LabelProp	–	0.545 ± 0.000	**0.598 ± 0.000**	0.962 ± 0.000
	LogReg	Adj	0.494 ± 0.003	0.455 ± 0.000	1.002 ± 0.003
	LogReg	LapEigMap	0.538 ± 0.007	0.596 ± 0.001	0.985 ± 0.023
	LogReg	SVD	0.545 ± 0.027	0.433 ± 0.005	0.721 ± 0.063
	LogReg	LINE1	0.608 ± 0.030	0.596 ± 0.030	**1.025 ± 0.040**
	LogReg	LINE2	0.575 ± 0.062	0.557 ± 0.018	1.017 ± 0.093
	LogReg	Node2vec	**0.633 ± 0.065**	0.500 ± 0.043	0.904 ± 0.078
	LogReg	Walklets	0.485 ± 0.071	0.458 ± 0.088	0.707 ± 0.069
OmniPath	GCN	OneHotLogDeg	**1.196 ± 0.054**	**0.983 ± 0.067**	**1.742 ± 0.107**
	SAGE	OneHotLogDeg	0.913 ± 0.074	0.779 ± 0.051	1.539 ± 0.074
	GIN	OneHotLogDeg	0.795 ± 0.044	0.731 ± 0.030	1.521 ± 0.086
	GAT	OneHotLogDeg	0.775 ± 0.142	0.773 ± 0.135	1.685 ± 0.110
	GatedGCN	OneHotLogDeg	1.112 ± 0.039	0.898 ± 0.031	1.698 ± 0.059
	LabelProp	–	**1.358 ± 0.000**	0.897 ± 0.000	1.593 ± 0.000
	LogReg	Adj	1.051 ± 0.001	0.709 ± 0.000	1.862 ± 0.000
	LogReg	LapEigMap	1.319 ± 0.000	**1.060 ± 0.004**	1.943 ± 0.004
	LogReg	SVD	0.866 ± 0.001	0.635 ± 0.006	1.512 ± 0.012
	LogReg	LINE1	0.834 ± 0.026	0.787 ± 0.007	1.893 ± 0.032
	LogReg	LINE2	0.913 ± 0.033	0.692 ± 0.012	1.844 ± 0.032
	LogReg	Node2vec	1.178 ± 0.035	0.924 ± 0.035	**2.125 ± 0.059**
	LogReg	Walklets	0.915 ± 0.041	0.795 ± 0.045	1.704 ± 0.064
ProteomeHD	GCN	OneHotLogDeg	0.690 ± 0.064	0.637 ± 0.066	**1.459 ± 0.138**
	SAGE	OneHotLogDeg	0.556 ± 0.107	0.644 ± 0.030	1.304 ± 0.041
	GIN	OneHotLogDeg	0.608 ± 0.083	0.606 ± 0.107	1.350 ± 0.221
	GAT	OneHotLogDeg	**0.705 ± 0.115**	0.687 ± 0.063	1.339 ± 0.199
	GatedGCN	OneHotLogDeg	0.521 ± 0.101	**0.712 ± 0.044**	1.169 ± 0.052
	LabelProp	–	0.709 ± 0.000	0.669 ± 0.000	1.036 ± 0.000
	LogReg	Adj	0.849 ± 0.047	0.619 ± 0.005	1.329 ± 0.141
	LogReg	LapEigMap	**0.955 ± 0.001**	0.721 ± 0.016	1.219 ± 0.039
	LogReg	SVD	0.878 ± 0.002	0.736 ± 0.008	**1.508 ± 0.079**
	LogReg	LINE1	0.566 ± 0.089	0.667 ± 0.023	1.307 ± 0.060
	LogReg	LINE2	0.576 ± 0.099	0.663 ± 0.032	1.226 ± 0.085
	LogReg	Node2vec	0.643 ± 0.076	**0.772 ± 0.068**	1.357 ± 0.040
	LogReg	Walklets	0.432 ± 0.050	0.525 ± 0.111	1.048 ± 0.061
SIGNOR	GCN	OneHotLogDeg	**1.387 ± 0.067**	**1.167 ± 0.079**	**1.732 ± 0.031**
	SAGE	OneHotLogDeg	0.924 ± 0.106	0.838 ± 0.086	1.441 ± 0.094
	GIN	OneHotLogDeg	1.106 ± 0.058	0.870 ± 0.055	1.479 ± 0.090
	GAT	OneHotLogDeg	1.180 ± 0.069	1.009 ± 0.087	1.576 ± 0.047
	GatedGCN	OneHotLogDeg	1.067 ± 0.028	0.852 ± 0.060	1.430 ± 0.085
	LabelProp	–	1.288 ± 0.000	1.096 ± 0.000	1.695 ± 0.000
	LogReg	Adj	1.303 ± 0.003	1.052 ± 0.001	1.417 ± 0.004
	LogReg	LapEigMap	1.306 ± 0.004	1.056 ± 0.005	1.746 ± 0.010
	LogReg	SVD	0.864 ± 0.004	0.801 ± 0.002	1.183 ± 0.002
	LogReg	LINE1	**1.412 ± 0.033**	0.955 ± 0.022	**1.781 ± 0.056**
	LogReg	LINE2	1.257 ± 0.034	0.917 ± 0.016	1.572 ± 0.047
	LogReg	Node2vec	1.341 ± 0.021	**1.172 ± 0.027**	1.684 ± 0.099
	LogReg	Walklets	1.017 ± 0.101	0.985 ± 0.049	1.259 ± 0.065

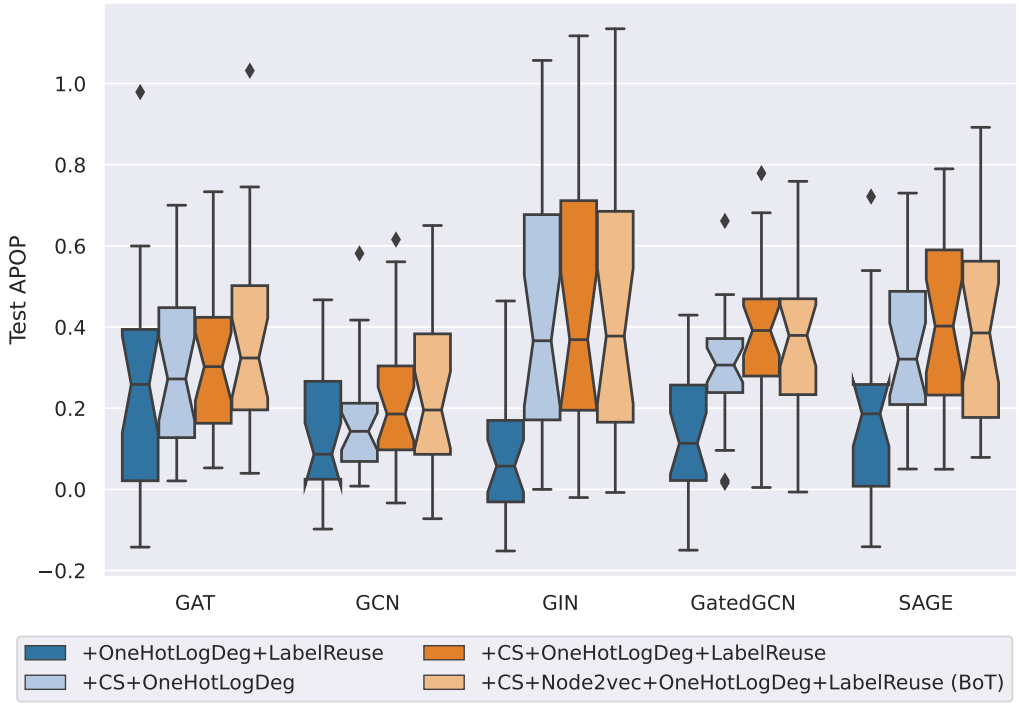

Figure S3: **Boxplots representing the performance improvement of using different tricks with GNNs across datasets.** Each point in a box is the test APOP difference of GNN with added tricks vs. plain GNN using OneHotLogDeg feature on a specific dataset. A positive value implies the added trick improves GNN performance.

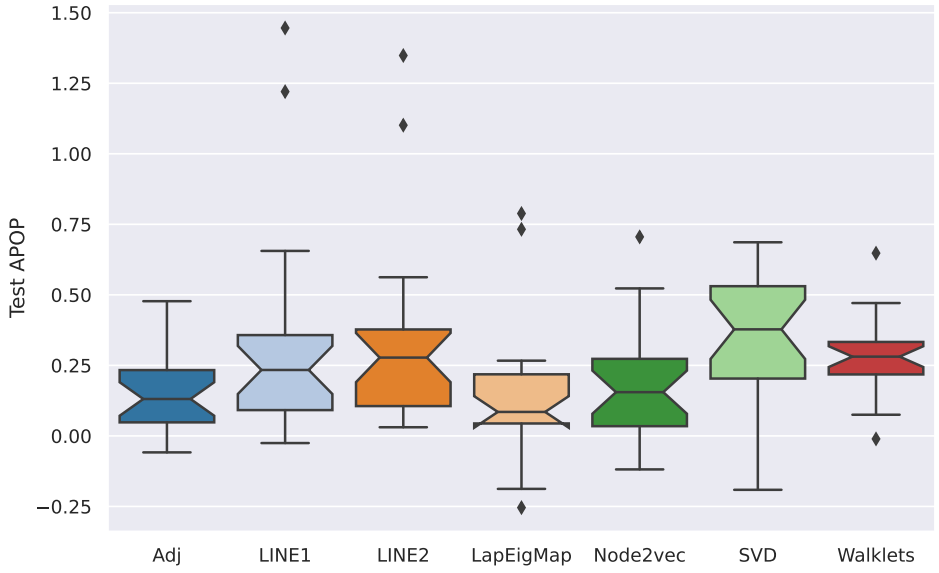

Figure S4: **Boxplots representing the performance improvement of using C&S with logistic regression models across datasets.** Each point in a box is the test APOP difference of logistic regression augmented with C&S vs. plain logistic regression on a specific dataset. A positive value implies C&S improves logistic regression performance.

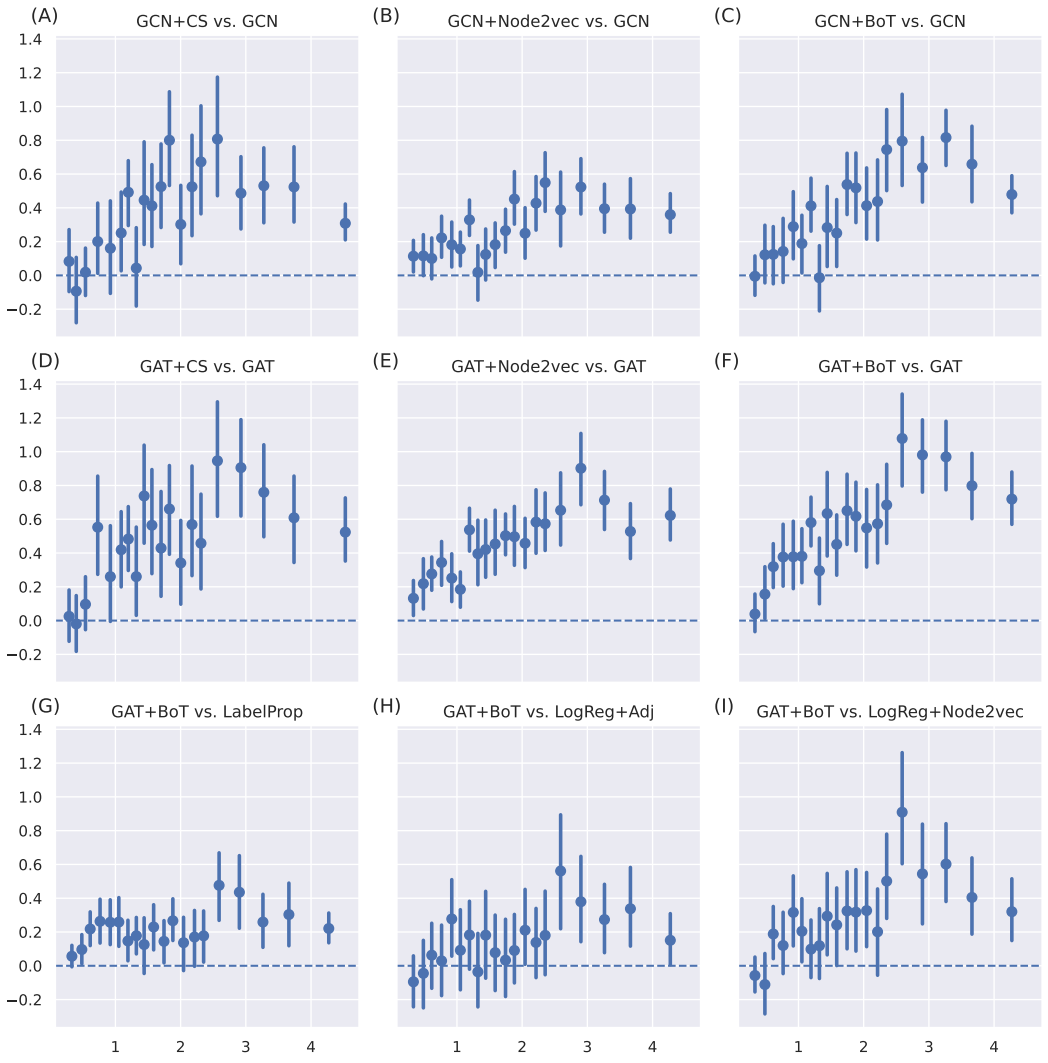

Figure S5: **Relationships between the corrected homophily ratio and performance difference between methods.** Each panel summarizes tasks over three networks (BioGRID, HumanNet, ComPPIHumanInt) and three gene set collections (DISEASES, DisGeNET, GOBP), with a total of 1,672 tasks. In each panel, the x-axis represents the corrected homophily ratio and the y-axis represents the test APOP performance difference between the two methods. The first (A, B, C) and second rows (D, E, F) show the performance improvement to GCN and GAT when augmented with individual tricks or combined BoT. The third row (G, H, I) shows the performance difference between the best GNN method and the baseline methods, including label propagation and logistic regression.

Table S7: Combined SOTA performance reference. LogReg* are the best test performances achieved from any logistic regression models we have tested for each dataset. Colored texts indicate the **first**, **second**, and **third** best performance achieved for a particular dataset (network × label).

Network	Model	DISEASES	DisGeNET	GOBP
BioGRID	LabelProp	1.210 ± 0.000	0.931 ± 0.000	1.885 ± 0.000
	LogReg*	**1.556 ± 0.002**	1.026 ± 0.022	**2.571 ± 0.015**
	GCN+BoT	1.511 ± 0.053	1.014 ± 0.020	2.411 ± 0.044
	SAGE+BoT	1.486 ± 0.058	**1.031 ± 0.049**	2.402 ± 0.061
	GIN+BoT	1.410 ± 0.024	1.007 ± 0.028	2.386 ± 0.022
	GAT+BoT	**1.609 ± 0.048**	**1.037 ± 0.036**	**2.624 ± 0.070**
	GatedGCN+BoT	**1.547 ± 0.027**	**1.038 ± 0.006**	**2.517 ± 0.047**
HumanNet	LabelProp	**3.728 ± 0.000**	3.059 ± 0.000	3.806 ± 0.000
	LogReg*	**3.812 ± 0.000**	**3.158 ± 0.000**	**4.053 ± 0.021**
	GCN+BoT	3.552 ± 0.050	3.053 ± 0.078	**3.921 ± 0.045**
	SAGE+BoT	3.401 ± 0.066	3.052 ± 0.041	3.816 ± 0.083
	GIN+BoT	3.513 ± 0.029	3.054 ± 0.051	3.861 ± 0.063
	GAT+BoT	**3.761 ± 0.060**	**3.100 ± 0.031**	**3.908 ± 0.086**
	GatedGCN+BoT	3.677 ± 0.066	**3.086 ± 0.020**	3.889 ± 0.048
ComPPIHumanInt	LabelProp	1.352 ± 0.000	1.106 ± 0.000	2.076 ± 0.000
	LogReg*	1.644 ± 0.006	**1.240 ± 0.009**	**2.806 ± 0.049**
	GCN+BoT	1.648 ± 0.012	1.211 ± 0.013	2.685 ± 0.047
	SAGE+BoT	**1.694 ± 0.055**	1.210 ± 0.033	2.629 ± 0.082
	GIN+BoT	1.608 ± 0.020	**1.219 ± 0.006**	2.611 ± 0.021
	GAT+BoT	**1.665 ± 0.035**	**1.230 ± 0.025**	**2.785 ± 0.041**
	GatedGCN+BoT	**1.672 ± 0.053**	1.218 ± 0.009	**2.735 ± 0.048**
BioPlex	LabelProp	0.964 ± 0.000	0.556 ± 0.000	2.174 ± 0.000
	LogReg*	**1.358 ± 0.006**	**0.939 ± 0.002**	**2.587 ± 0.022**
	GCN+BoT	1.324 ± 0.027	**0.911 ± 0.010**	**2.553 ± 0.069**
	SAGE+BoT	1.246 ± 0.022	0.865 ± 0.035	2.513 ± 0.038
	GIN+BoT	**1.349 ± 0.010**	0.868 ± 0.009	2.504 ± 0.024
	GAT+BoT	**1.355 ± 0.040**	**0.873 ± 0.025**	2.548 ± 0.075
	GatedGCN+BoT	1.301 ± 0.035	0.859 ± 0.011	**2.590 ± 0.029**
HuRI	LabelProp	0.545 ± 0.000	0.598 ± 0.000	0.962 ± 0.000
	LogReg*	**0.650 ± 0.000**	0.656 ± 0.000	1.084 ± 0.020
	GCN+BoT	**0.634 ± 0.065**	**0.693 ± 0.019**	**1.229 ± 0.119**
	SAGE+BoT	0.593 ± 0.040	0.679 ± 0.031	**1.190 ± 0.127**
	GIN+BoT	0.583 ± 0.042	**0.702 ± 0.012**	1.143 ± 0.047
	GAT+BoT	**0.667 ± 0.048**	0.687 ± 0.045	1.174 ± 0.047
	GatedGCN+BoT	0.596 ± 0.017	**0.695 ± 0.018**	**1.195 ± 0.054**
OmniPath	LabelProp	1.358 ± 0.000	0.897 ± 0.000	1.593 ± 0.000
	LogReg*	**1.542 ± 0.017**	**1.093 ± 0.006**	**2.125 ± 0.059**
	GCN+BoT	**1.577 ± 0.038**	1.073 ± 0.024	2.052 ± 0.032
	SAGE+BoT	1.465 ± 0.048	1.041 ± 0.065	1.974 ± 0.040
	GIN+BoT	1.478 ± 0.032	**1.104 ± 0.017**	1.995 ± 0.046
	GAT+BoT	1.520 ± 0.028	**1.083 ± 0.025**	**2.067 ± 0.050**
	GatedGCN+BoT	**1.544 ± 0.036**	1.079 ± 0.020	**2.122 ± 0.080**
ProteomeHD	LabelProp	0.709 ± 0.000	0.669 ± 0.000	1.036 ± 0.000
	LogReg*	**0.955 ± 0.001**	**0.776 ± 0.000**	**1.519 ± 0.071**
	GCN+BoT	0.764 ± 0.017	**0.745 ± 0.026**	1.387 ± 0.088
	SAGE+BoT	0.747 ± 0.051	**0.734 ± 0.023**	1.425 ± 0.100
	GIN+BoT	0.771 ± 0.034	0.718 ± 0.029	**1.529 ± 0.161**
	GAT+BoT	**0.830 ± 0.039**	0.727 ± 0.042	**1.463 ± 0.052**
	GatedGCN+BoT	**0.829 ± 0.029**	0.716 ± 0.022	1.389 ± 0.097
SIGNOR	LabelProp	1.288 ± 0.000	1.096 ± 0.000	1.695 ± 0.000
	LogReg*	1.582 ± 0.006	**1.298 ± 0.007**	**1.894 ± 0.001**
	GCN+BoT	**1.590 ± 0.037**	**1.273 ± 0.013**	1.844 ± 0.031
	SAGE+BoT	1.540 ± 0.017	1.243 ± 0.005	1.784 ± 0.041
	GIN+BoT	**1.593 ± 0.026**	1.253 ± 0.010	**1.850 ± 0.028**
	GAT+BoT	**1.627 ± 0.042**	**1.260 ± 0.009**	1.799 ± 0.034

GatedGCN+BoT	1.525 ± 0.026	1.254 ± 0.006	**1.849 ± 0.029**

Table S8: Random splitting evaluation performance of different methods on the four primary OBNB datasets evaluated in APOP ↑ aggregated over five seeds. **Bold** indicates the best-performing method within the method class (traditional ML or GNN). Blue indicates the evaluated performance is higher than the study-biased holdout evaluation counterpart.

			BioGRID		HumanNet	
Model	Features	C&S?	DisGeNET	GOBP	DisGeNET	GOBP
LabelProp	–	✗	1.415 ± 0.000	2.654 ± 0.000	**3.370 ± 0.000**	4.138 ± 0.000
LogReg	Adj	✗	**1.546 ± 0.001**	**3.479 ± 0.000**	3.280 ± 0.000	**4.300 ± 0.001**
LogReg	N2V	✗	1.485 ± 0.037	3.269 ± 0.022	2.987 ± 0.014	4.107 ± 0.033
LogReg	LapEigMap	✗	1.421 ± 0.000	2.812 ± 0.004	2.516 ± 0.002	3.876 ± 0.004
GCN	LogDeg	✗	1.055 ± 0.116	2.076 ± 0.204	2.770 ± 0.045	3.898 ± 0.063
GCN	LogDeg	✓	1.664 ± 0.066	2.832 ± 0.082	3.213 ± 0.010	4.134 ± 0.044
GCN†	N2V+LogDeg+Label	✓	1.780 ± 0.043	3.330 ± 0.049	**3.278 ± 0.023**	4.205 ± 0.030
GCN‡	N2V+LogDeg+Label	✓	1.769 ± 0.051	3.380 ± 0.047	3.274 ± 0.013	4.202 ± 0.023
GAT	LogDeg	✗	0.921 ± 0.290	2.722 ± 0.498	2.837 ± 0.197	3.838 ± 0.092
GAT	LogDeg	✓	1.791 ± 0.015	3.076 ± 0.037	3.252 ± 0.021	4.141 ± 0.016
GAT†	N2V+LogDeg+Label	✓	1.728 ± 0.063	3.357 ± 0.185	3.265 ± 0.018	4.226 ± 0.030
GAT‡	N2V+LogDeg+Label	✓	**1.818 ± 0.013**	**3.448 ± 0.010**	3.266 ± 0.003	**4.235 ± 0.020**

† recommended BoT, ‡ recommended BoT with fully tuned GNNs (see Appendix A.4.1 for tuning details)

As shown in Table S8, random-split performance is higher than study-biased holdout in all cases. This indicates that, besides being more realistic, the study-biased holdout split is a much harder evaluation scheme and thus provides a more stringent evaluation of the tested gene classification method.

Table S9: Task-specific model prediction performance difference on the BioGRID-DisGeNET between GAT and LogReg+Adj.

Task ID	Task Name	GAT	LogReg+Adj	Difference
MONDO:0002289	Iris disorder	2.160	0.149	2.011
MONDO:0001703	Color-vision disease	2.177	0.230	1.946
MONDO:0001926	Ureteral disorder	1.543	-0.336	1.879
MONDO:0005552	Ocular vascular disease	1.507	-0.175	1.682
MONDO:0018470	Renal agenesis	1.273	-0.347	1.620
…				
MONDO:0020018	Cranial malformation	0.699	4.487	-3.788
MONDO:0019743	Nephropathy secondary to a storage or other metabolic disease	0.773	4.876	-4.103
MONDO:0024757	Cardiovascular neoplasm	0.316	4.443	-4.127
MONDO:0045011	Keratinization disease	0.264	4.619	-4.355
MONDO:0015160	Multiple congenital anomalies/dysmorphic syndrome-variable intellectual disability syndrome	0.280	4.828	-4.549

Table S11: Statistics for all datasets in OBNB (`obnbdata-0.1.0`)

Label	Network	Num. tasks	Num. pos. avg.	Num. pos. std.	Num. pos. med.
DISEASES	BioGRID	145	178.1	137.4	127.0
	BioPlex	72	123.8	64.4	101.5
	ComPPIHumanInt	145	174.6	134.5	125.0
	ConsensusPathDB	144	177.4	137.5	126.0
	FunCoup	145	177.1	135.1	127.0
	HIPPIE	143	178.1	137.6	127.0
	HuMAP	123	168.0	119.2	120.0
	HuRI	50	130.3	56.7	112.5
	HumanBaseTopGlobal	149	178.5	137.7	129.0
	HumanNet	142	179.0	136.9	127.0
	OmniPath	135	180.2	131.1	131.0
	PCNet	143	171.8	130.6	122.0
	ProteomeHD	15	76.9	22.4	70.0
	SIGNOR	89	144.6	89.4	117.0
	STRING	146	175.4	135.6	126.0
DisGeNET	BioGRID	305	208.3	143.1	159.0

	BioPlex	189	138.6	71.4	111.0
	ComPPIHumanInt	301	204.1	138.7	159.0
	ConsensusPathDB	298	207.4	140.8	161.5
	FunCoup	299	204.7	139.4	158.0
	HIPPIE	306	208.1	142.9	159.5
	HuMAP	279	194.3	126.7	155.0
	HuRI	152	122.9	54.7	108.0
	HumanBaseTopGlobal	287	219.7	145.7	173.0
	HumanNet	302	204.2	140.3	158.5
	OmniPath	298	199.6	136.0	153.5
	PCNet	292	202.1	135.5	159.0
	ProteomeHD	56	78.0	24.8	71.0
	SIGNOR	219	147.3	81.9	124.0
	STRING	296	208.0	140.6	162.0
GOBP	BioGRID	114	89.5	37.1	76.0
	BioPlex	38	77.6	22.6	76.0
	ComPPIHumanInt	104	91.8	37.0	77.5
	ConsensusPathDB	112	90.1	37.0	76.5
	FunCoup	114	87.8	36.7	74.0
	HIPPIE	111	89.2	37.1	76.0
	HuMAP	96	84.6	32.3	74.0
	HuRI	27	69.9	16.0	65.0
	HumanBaseTopGlobal	115	89.2	37.3	76.0
	HumanNet	117	88.6	36.9	75.0
	OmniPath	106	88.7	36.2	74.0
	PCNet	105	89.0	36.0	77.0
	ProteomeHD	5	80.4	22.6	70.0
	SIGNOR	41	81.3	22.7	78.0
	STRING	116	88.9	36.6	75.0
GOCC	BioGRID	71	96.0	36.3	87.0
	BioPlex	35	77.0	20.9	71.0
	ComPPIHumanInt	68	96.1	35.5	88.0
	ConsensusPathDB	71	95.5	35.8	87.0
	FunCoup	71	95.9	36.4	87.0
	HIPPIE	69	97.3	35.8	89.0
	HuMAP	62	91.8	33.4	82.0
	HuRI	21	69.0	12.4	67.0
	HumanBaseTopGlobal	71	96.9	36.3	88.0
	HumanNet	70	95.8	35.6	88.0
	OmniPath	67	94.0	34.6	84.0
	PCNet	70	93.5	35.0	85.0
	ProteomeHD	2	59.5	4.5	59.5
	SIGNOR	26	66.4	11.3	67.5
	STRING	69	96.1	35.6	88.0
GOMF	BioGRID	63	97.7	39.8	85.0
	BioPlex	25	79.6	18.0	79.0
	ComPPIHumanInt	62	98.1	39.7	86.0
	ConsensusPathDB	63	98.2	39.5	85.0
	FunCoup	64	97.5	39.1	83.5
	HIPPIE	63	97.7	39.9	84.0
	HuMAP	58	92.1	36.8	74.5
	HuRI	22	74.8	12.8	73.5
	HumanBaseTopGlobal	62	99.2	39.9	86.0
	HumanNet	61	98.7	39.5	84.0
	OmniPath	64	95.2	38.5	83.5
	PCNet	58	97.4	38.6	86.0
	ProteomeHD	2	59.5	4.5	59.5
	SIGNOR	25	91.4	23.7	94.0
	STRING	62	98.0	39.3	82.5

Table S10: Statistics for all networks in OBNB (`obnbdata-0.1.0`)

Network	Weighted	Num. nodes	Num. edges	Density	Category
HumanBaseTopGlobal [29]	✓	25,689	77,807,094	0.117908	Large & Dense
HuMAP [20]	✓	15,433	35,052,604	0.147180	Large & Dense
STRING [86]	✓	18,480	11,019,492	0.032269	Large
ConsensusPathDB [46]	✓	17,735	10,611,416	0.033739	Large
FunCoup [76]	✓	17,892	10,037,478	0.031357	Large
PCNet [36]	✗	18,544	5,365,116	0.015603	Large
BioGRID [85]	✗	19,765	1,554,790	0.003980	Medium
HumanNet [42]	✓	18,591	2,250,780	0.006513	Medium
HIPPIE [1]	✓	19,338	1,542,044	0.004124	Medium
ComPPIHumanInt [92]	✓	17,015	699,620	0.002417	Medium
OmniPath [88]	✗	16,325	289,134	0.001085	Small
ProteomeHD [50]	✗	2,471	125,172	0.020509	Small
HuRI [60]	✗	8,100	103,188	0.001573	Small
BioPlex [41]	✗	8,108	71,004	0.001080	Small
SIGNOR [73]	✗	5,291	28,676	0.001025	Small